Atmos. Chem. Phys. Discuss., 11, 26347–26413, 2011
www.atmos-chem-phys-discuss.net/11/26347/2011/
doi:10.5194/acpd-11-26347-2011

Atmospheric Chemistry and Physics Discussions

Global mechanistic model of SOA formation: effects of different chemical mechanisms

G. Lin[1], J. E. Penner[1], S. Sillman[1], D. Taraborrelli[2], and J. Lelieveld[2,3]

[1]Department of Atmospheric, Oceanic, and Space Sciences, University of Michigan, Ann Arbor, Michigan, USA
[2]Department of Atmospheric Chemistry, Max Planck Institute for Chemistry, Mainz, Germany
[3]The Cyprus Institute, Nicosia, Cyprus

Received: 5 August 2011 – Accepted: 7 September 2011 – Published: 22 September 2011

Correspondence to: G. Lin (gxlin@umich.edu)

Published by Copernicus Publications on behalf of the European Geosciences Union.

Abstract

Recent experimental findings indicate that Secondary Organic Aerosol (SOA) represents an important and, under many circumstances, the major fraction of the organic aerosol burden. Here, we use a global 3-d model (IMPACT) to test the results of different mechanisms for the production of SOA. The basic mechanism includes SOA formation from organic nitrates and peroxides produced from an explicit chemical formulation, using partition coefficients based on thermodynamic principles. We also include the formation of non-evaporative SOA from the reaction of glyoxal and methylglyoxal on aqueous aerosols and cloud droplets as well as from the reaction of epoxides on aqueous aerosols. A model simulation including these SOA formation mechanisms gives an annual global SOA production of 113.5 Tg. The global production of SOA is substantially decreased to 85.0 Tg yr^{-1} if the HO_x regeneration mechanism proposed by Peeters et al. (2009) is used. Model predictions with and without this HO_x regeneration scheme are compared with multiple surface observation datasets, namely: the Interagency Monitoring of Protected Visual Environments (IMPROVE) for the United States, the European Monitoring and Evaluation Programme (EMEP) as well as Aerosol Mass Spectrometry (AMS) data measured in both Northern Hemisphere and tropical forest regions. All model simulations realistically predict the organic carbon mass observed in the Northern Hemisphere, although they tend to overestimate the concentrations in tropical forest regions. This overestimate may result from an unrealistically high uptake rate of glyoxal and methylglyoxal on aqueous aerosols and in cloud drops. The modeled OC in the free troposphere is in agreement with measurements in the ITCT-2K4 aircraft campaign over the North America and in pollution layers in Asia during the INTEX-B campaign, although the model underestimates OC in the free troposphere during the ACE-Asia campaign off the coast of Japan.

ACPD
11, 26347–26413, 2011

1 Introduction

Atmospheric particles have important impacts on human health, air quality and the regional to global climate. Organic aerosols represent a large fraction of the particulate mass at both urban and remote locations (Kanakidou et al., 2005; Zhang et al., 2007; Jimenez et al., 2009). They are often categorized as either "primary organic aerosol (POA)", a class of organic compounds that is emitted directly into the atmosphere in particulate form, or "secondary organic aerosols (SOA)", which are formed by atmospheric oxidation of volatile organic compounds (VOCs).

Despite the importance of organic aerosols (OA) on the environment, data sets to constrain models are limited. Nevertheless, based on available data sets it appears that models tend to underestimate SOA concentrations in the boundary layer (e.g., Johnson et al., 2006; Volkamer et al., 2006; Kleinman et al., 2008; Simpson et al., 2007) as well as in the free troposphere (Heald et at., 2005). Johnson et al.(2006) studied SOA formation in the UK using fully explicit chemical schemes in the modified Master Chemical Mechanism (MCM v3.1), and found that they had to increase all partitioning coefficients of SOA precursors by a factor of 500 in order to capture observed OA levels. Volkamer et al. (2006) employed aerosol mass spectrometer (AMS) measurements to analyze the surface concentrations of oxidized organic aerosol (OOA) in Mexico City. The measured SOA was about 8 times larger than a conservative (high end) estimate from an SOA model based on an empirical parameterization of chamber experiments. Their results were corroborated by Kleinman et al. (2008) who reported a similar discrepancy of an order of magnitude higher measured SOA than that computed by a model for Mexico City, using aircraft data from the MILAGRO 2006 campaign. Simpson et al. (2007) found that their SOA modeling framework under-predicted SOA concentrations at European sites. Heald et al. (2005) compared free tropospheric OA measurements from the Asia Pacific Regional Aerosol Characterization Experiment (ACE-Asia) field campaign with predictions from the global chemical transport model GEOS-Chem and concluded that a significant source of SOA was missing in the free

ACPD
11, 26347–26413, 2011

troposphere.

Although these regional and global models showed a tendency to under-predict organic carbon (OC) concentrations in polluted regions, there is no universal underestimation for regions in which biogenic sources dominate (Capes et al., 2009; Chen et al., 2009; Slowik et al., 2010). Capes et al. (2009) presented measurements of OA over subtropical West Africa during the wet season using data from the UK Facility for Airborne Atmospheric Measurements (FAAM) aircraft. Their theoretical SOA estimates based on aerosol yields from isoprene and monoterpenes under-represented the organic matter (OM) measured in this region to an extent roughly consistent with that in polluted environments. Chen et al. (2009) showed only 35 % lower organic loadings of GEOS-Chem simulations than measurements in the Amazon Basin taken using a high-resolution AMS during the wet season of 2008. In contrast to model under predictions reported in polluted regions, Slowik et al. (2010) obtained very good agreement for biogenic SOA concentrations between measurements and regional air quality model simulations of eastern Canadian forest regions.

The reasons for the differences between measured vs. modeled SOA in different regions remain unclear due to the numerous and complex chemical and physical phenomena involved in SOA formation (Hallquist et al., 2009; Pankow and Barsanti, 2009). One major uncertainty relates to the gaseous secondary organics. It has been estimated that there are many hundreds of thousands of different organic compounds in the atmosphere (Goldstein and Galbally, 2007), with each compound further undergoing a number of atmospheric reactions to produce a range of oxidized products (Hallquist et al., 2009). Therefore, the atmosphere contains a highly complex mixture of a myriad of structurally different organic oxygenates with a wide range of physical-chemical properties, with different gas-to-particle-transfer potentials (Utembe et al., 2011; Lee-Talor et al., 2011).The complexity of the emitted VOC mixture and the degradation chemistry requires a rigorous and thorough gas-phase chemical mechanism that describes SOA formation. Globally, isoprene emissions (~500 Tg C yr^{-1}) (Guenther et al., 2006) constitute around one third of total VOC emissions to the atmosphere

ACPD
11, 26347–26413, 2011

(Goldstein and Galbally, 2007). As a consequence, SOA derived from biogenic VOCs dominate the predicted global atmospheric SOA burden (Chuang and Seinfeld, 2002: Tsigarids et al., 2006; Henze et al., 2008) and some measured data also suggest that most of the SOA is indeed associated with biogenic emissions (Lewis et al, 2004; Kleindienst et al, 2007; Szidat et al., 2009; Goldstein et al., 2009). However, the precise mechanisms of the SOA formation are not known. Recently, field studies in forested environments have found much higher OH radical concentrations than model predictions based on traditional mechanisms in which isoprene hydroxyperoxy radicals react mainly with HO_2 to form organic hydroperoxides in low NO_x conditions (Lelieveld et al., 2008; Pugh et al., 2010). This indicates that the isoprene oxidation mechanisms traditionally used in chemistry-transport models may require substantial revision.

In addition to the degradation mechanisms for VOCs, other efforts have focused on the gap between measured and modeled SOA. What has traditionally been considered non-volatile primary organic aerosol (POA) from diesel exhaust and biomass burning is recently claimed to be a dynamic system of semi-volatile species which can partition between the gas and aerosol phase as well as undergo gas-phase oxidation to form species of different volatilities that can condense to form SOA (Robinson et al., 2007; Huffman et al., 2009). This previously neglected new SOA source has been explored in several box (Dzepina et al., 2009), regional (Hodzic et al., 2010) and global (Pye and Seinfeld, 2010) modeling studies, which indicate that such new sources may be important in modeling regional and global SOA formation. However, there is still substantial uncertainty in the emissions, reaction rates, and SOA yields of primary emitted VOCs with relatively low volatility (Pye and Seinfeld, 2010; Spracklen et al., 2011).

While the volatility of the gas-phase products formed is important in driving the SOA formation from VOC degradation, the propensity of oxidation products to undergo further reactions within or on the condensed phase has also been established to play a key role in the formation and growth of SOA over the last 5–10 years. Condensed-phase reactions can cause the vapor pressure of organics to be lowered by several orders of magnitude either by oxidation or by the formation of high-molecular-weight

ACPD
11, 26347–26413, 2011

species (e.g., through oligomerization) (Hallquist et al., 2009).The rate of formation of these low volatility compounds increases in the presence of inorganic acid seed aerosol, at least for the products formed in the ozonolysis of alpha-pinene (Jang et al., 2006; Czoschke et al, 2003; Iinuma et al., 2004; Gao et al., 2004a, 2004b). Additionally, in regions where isoprene is present acidic sulphate aerosols may lead to the formation of epoxydiols (Paulot et al., 2009) and their reactive uptake (Minerath and Elrod, 2009) may lead to a 20-fold increase in OA mass yields from isoprene (Surratt et al., 2010). Similarly, the uptake of gas-phase glyoxal into aqueous ammonium sulfate particles was also observed (Jang and Kamens, 2001; Hastings et al., 2005; Kroll et al., 2005b; Liggio et al., 2005a). Following this observation, the production of glyoxal as well as methylglyoxal together with the formation of SOA has been examined in a global model (Fu et al., 2008).

In this paper, we begin with a model description in Sect. 2, describing the gas-phase chemical mechanisms for oxidation of VOCs and SOA formation mechanisms for gas-particle partitioning of SVOCs and for irreversible uptake of glyoxal, methylglyoxal and epoxydiols. Our model results using different chemical mechanisms are presented in Sect. 3. Section 4 compares our model simulations with both surface and free troposphere observations. Finally, a summary is presented in Sect. 5.

2 Model description

Here, we use the Integrated Massively Parallel Atmospheric Chemical Transport (IMPACT) model that was developed at the Lawrence Livermore National Laboratory (LLNL) (Rotman et al., 2004) and at the university of Michigan (Penner et al., 1998; Liu and Penner, 2002; Liu et al., 2005; Ito et al., 2007).The IMPACT model was developed using massively parallel computer architecture and was extended by Liu and Penner (2002) to treat the mass of sulfate aerosol as a prognostic variable. It was further extended by Liu et al. (2005) to treat the microphysics of sulfate aerosol and the interactions between sulfate and non-sulfate aerosols based on the aerosol module

ACPD
11, 26347–26413, 2011

developed by Herzog et al. (2004). Ito et al. (2007) investigated the effect of non-methane volatile organic compounds on tropospheric ozone and its precursors using the IMPACT model, with a modified numerical solution for photochemistry (Sillman, 1991) and a modified chemical mechanism (Ito et al., 2007). In this work, we also use the 1997 meteorological fields from the National Aeronautics and Space Administration (NASA) Data Assimilation Office (DAO) GEOS-START (Goddard EOS Assimilation System-Stratospheric Tracers of Atmospheric Transport) model (Coy and Swinbank, 1997; Coy et al., 1997). The meteorology was defined on a 4° latitude × 5 °longitude horizontal grids with 46 vertical layers. The model was run for a 1-year time period with a 1-month spin up time.

2.1 Atmospheric degradation mechanisms of SOA precursors

2.1.1 Chemical mechanism by Ito et al. (2007)

We used the chemical mechanism published by Ito et al. (2007) to represent the basic photochemistry of O_3, OH, NO_x and volatile organic compounds (VOC). The Ito mechanism uses surrogate species to represent classes of VOC, so that (for example) the chemistry of toluene is also used to represent ethyl benzene. Representation of chemical reaction pathways to form SOA described below, are all incorporated into the Ito gas-phase mechanism. In certain cases we have used modified reaction sequences (e.g. Peeters et al. (2009), for the first stages of isoprene oxidation) as replacements for the original sequences from Ito et al. (2007), as described below. In these cases the subsequent reaction products (e.g. methylvinyl ketone) react as in Ito et al. (2007), unless otherwise specified. The gas-phase oxidation is initiated by reaction with hydroxyl (OH) radicals, O_3, nitrate (NO_3) radicals or via photolysis, leading to the formation of organic peroxy radicals (RO_2). In the presence of nitrogen oxides ($NO_x = NO + NO_2$), RO_2, oxy radicals (RO) and the hydroperoxy radical (HO_2) can act as chain propagating species, leading to the regeneration of OH (e.g., Kroll and Seinfeld, 2008). The reactions of RO_2 and HO_2 with NO play a key role in these catalytic cycles, since the

ACPD
11, 26347–26413, 2011

associated oxidation of NO to NO_2 leads to the formation of ozone by the subsequent photolysis of NO_2:

$$RO_2 + NO \longrightarrow RO + NO_2 \quad \text{(R1)}$$

$$HO_2 + NO \longrightarrow OH + NO_2 \quad \text{(R2)}$$

At low levels of NO_x, RO_2 will instead react with HO_2 and then form a hydroperoxide, leading to a general suppression of the concentrations of the free radical species:

$$RO_2 + HO_2 \longrightarrow ROOH + O_2 \quad \text{(R3)}$$

2.1.2 Epoxide formation following Paulot et al. (2009)

The gas-phase formation of epoxides (IEPOX) has been characterized by Paulot et al. (2009). These compounds are formed in the OH-initiated oxidation of isoprene hydroperoxide (RIP) under low-NO_x conditions. IEPOX formation is accompanied by OH regeneration and is implemented in the model as shown below:

$$RIP + OH \longrightarrow IEPOX + OH \quad \text{(R4)}$$

The subsequent oxidation of IEPOX is as follows:

$$IEPOX + OH \longrightarrow IEPOXO2 \quad \text{(R5)}$$

$$IEPOX + NO \longrightarrow NO_2 + 0.75HAC + 0.275GLYC + 0.275GLYX + 0.275MGLY \quad \text{(R6)}$$

$$+0.375HCHO + 0.074ACO2 + 0.251CO \quad \text{(R7)}$$

$$IEPOX + HO_2 \longrightarrow 0.825HO_2 + 0.125OH + 0.725HAC + 0.275GLYC + 0.275MGLY \quad \text{(R8)}$$

$$+0.375HCHO + 0.074ACO2 + 0.251CO \quad \text{(R9)}$$

ACPD
11, 26347–26413, 2011

2.1.3 HO_x regeneration in isoprene oxidation from Peeters et al. (2009)

As described in the Introduction, analysis of recent direct measurements of HO_x (OH and HO_2) over the Amazonian rainforest (Lelieveld et al., 2008) and the tropical forests of Borneo (Pugh et al., 2010) showed that the traditional chemistry used in numerical model studies cannot explain the high measured OH concentrations, which suggested that there is a yet unknown recycling mechanism for OH. To address this HO_x recycling issue, Peeters et al. (2009) proposed and theoretically quantified a novel HO_x-regenerating pathway for the OH-initiated oxidation of isoprene. This oxidation mechanism has the following main features. The isoprene hydroxyl alkyl radicals first react with O_2 to form three isoprene peroxyradicals, which are in near-equilibrium steady-state. Some of the isoprene peroxy radicals, i.e. β-peroxys, are proposed to undergo 1,5-H shifts, that compete with the conventional reaction channels through HO_2, RO_2 and NO, leading to OH and HCHO along with either methacrolein (MACR) or methylvinylketone (MVK). Similarly, the Z-δ-OH-peroxys may undergo fast 1,6-H shifts leading to the formation of HO_2 and hydroperoxy aldehydes, which can rapidly photodissociate, initiating a reaction cascade that can yield 1-3 OH radicals. Our simplified representation of the HO_x recycling mechanism is detailed in the Supplement.

Although the chemical mechanism framework proposed by Peeters et al. (2009) provides a significant potential for addressing the atmospheric OH recycling issue, some atmospheric field measurements (e.g., Karl et al., 2009) and laboratory data (e.g., Paulot et al., 2009) indicate that it does not fully capture all observations. Compared to field measurements conducted during the Amazonian Aerosol Characterization Experiment (AMAZE-08), Karl et al. (2009) pointed out that the Peeters et al. (2009) mechanism overestimates MVK/MACR ratios and under-predicts the sum of MVK and MACR relative to isoprene. Unrealistically high ratios of MVK/MACR and PAN/MPAN were also reported by Archibald et al. (2010) using the Peeters et al. (2009) mechanism. In addition, Paulot et al. (2009) carried out a chamber experiment and found a lower yield (<10 %) for the formation of the hydroperoxy-methyl-butenal isomers

ACPD
11, 26347–26413, 2011

(HPC41CHO and HPC42CHO) than that proposed by Peeters et al. (2009). Moreover, Da Silva et al. (2010) used density functional theory (DFT) methods to calculate the 1,5-H atom shift isomerization rates for the isoprene-derived β-peroxy radicals and obtained an order of magnitude lower rates than those reported by Peeters et al. (2009). To reconciles the differences between Peeters et al. (2009) and some other atmospheric observations or the laboratory data mentioned above, both Karl et al. (2009) and Archibald et al. (2010) decreased the 1,5-H shift, 1,6-H shift rates by a factor of 10 as a sensitivity test. However, Peeters and Mueller (2010) showed that Paulot et al. (2009) did not account for 25 % of the isoprene peroxy radicals produced during the experiments. Keeping this in mind, we also slow the 1,5-H and 1,6-H shift rates by a factor of 10 as a sensitivity simulation. During the preparation of this manuscript, an experimental estimate for 1,6-H shift was published (Crounse et al., 2011) being a factor of 50 $\pm$25 lower than the estimate of Peeters and Mueller (2010). Therefore, we carried out three different simulations with different gas-phase chemical mechanisms (see Table 1). Simulation A only employs the Ito et al. (2007) chemical mechanism together with the epoxide formation mechanism from Paulot et al. (2009). Simulation B includes the HO_x recycling mechanism during isoprene oxidation from Peeters et al. (2009) and the mechanism in the Simulation A with some reactions modified in accordance with the recent literature (refer to the Supplement). Simulation C uses the same chemical mechanism as Simulation B, but with the 1,5-H and 1,6-H shift rates reduced by a factor 10.

2.2 SOA formation

2.2.1 Gas-particle partitioning of semi-volatile organic compounds

Traditionally, SOA is considered to be formed through gas-particle partitioning of semi-volatile organic compounds. We call these SOA as ne_oSOA hereafter in this paper (see Table 1). "Ne" stands for "non-evaporative", and "oSOA" means "other oxidative SOA" to differentiate from SOA formed from the uptake of glyoxal, methylglyoxal and

ACPD
11, 26347–26413, 2011

epoxide which will be described in Sect. 2.2.2. The gas-particle partitioning of organics produced during gas-phase oxidation is based on the absorptive model described by Pankow (1994), which assumes thermodynamic equilibrium of gaseous oxidation products between the gas and particulate phase. According to this model, partitioning of each semi-volatile organic compound between the gas and aerosol phases can be described by an equilibrium partitioning coefficient K ($m^3 \mu g^{-1}$), or equivalently, its inverse, the effective saturation vapor concentration, C^* ($\mu g\, m^{-3}$), (Donahue et al., 2006),

$$\frac{[A_i]}{[G_i]} = K_i C_{OM} = \frac{C_{OM}}{C^*} \quad (1)$$

where C_{OM} is the mass concentration per unit volume of air of the total absorbing particle phase, which may include the pre-existing organic aerosol into which semi-volatile organics partition and possibly the aqueous portion of the organics if the semi-volatile organics are water-soluble. Here, we assume,

$$C_{OM} = [POA] + \sum_{i=1}^{n} [A_i] \quad (2)$$

In this equation n is the number of species that can partition to the aerosol phase, $[A_i]$ ($\mu g\, m^{-3}$) and $[G_i]$ ($\mu g\, m^{-3}$) are the concentrations of species i in the aerosol and gas phases, respectively. [POA] ($\mu g\, m^{-3}$) is the concentration of primary organic aerosols, though the inclusion of the latter may tend to overestimate the yield of SOA (Song et al., 2007).

In the first basic model of SOA formation in smog chambers using partitioning theory, Odum et al. (1996) fit the yields obtained from the chamber studies by assuming that the oxidation of a single parent hydrocarbon only formed two semi-volatile products. This two-product model has been employed in a number of regional and global models (Chung and Seinfeld, 2002; Tsigaridis and Kanakidou, 2003; Liao et al., 2007; Carlton et al., 2010). These types of models can include the effect of changes in NO_x emissions on O_3, and the effects of NO_x on the abundance of reaction products by fitting to smog

ACPD
11, 26347–26413, 2011

chamber results in high and low NO_x environments (Tsidigaris et al., 2006; Henze et al., 2008) and can also be extended to include more than two volatility products (Donahue, 2009).

However, the two-product representation assumes that SVOC is only produced from a single oxidation step of the parent hydrocarbon. Actually, SVOC formation is expected to be more complex and dynamic than arising from first generation oxidation products of a given precursor, with the possibility of multiple oxidation steps (Ng et al., 2006; Camredon et al., 2007; Kroll and Seinfeld, 2008). In addition, the experiments on which this empirical representation for SOA formation is built have often been carried out at levels of NO_x and hydrocarbon that are significantly higher than for typical tropospheric conditions (Kroll et al., 2007; Camredon et al., 2007; Hallquist et al., 2009), which compromises the ability to validate the formation mechanism in the atmosphere.

In contrast to this empirical Odum-type model, a second type of model uses an explicit photochemical mechanism to form SVOC (e.g. Griffin et al., 2002; Zhang et al., 2004; Pun et al., 2006; Johnson et al., 2006; Camredon et al., 2007; Xia et al., 2008; Utembe et al., 2011), but may be limited in its ability to form SOA if the product distribution is incorrect. Nevertheless, because this type of mechanism is more explicit in its description of the oxidation products that lead to SOA formation, we follow this philosophy here.

In this explicit model, a detailed gas-phase mechanism is used to predict the formation of semivolatile products, with gas-particle partitioning computed from an explicit calculation of K_i for each semivolatile compound. To determine the semivolatile compounds that might partition into the aerosol phase, we used the following criteria suggested by Griffin et al. (2002).

Partially soluble

An aromatic acid

An aromatic compound with two functional groups that are not aldehydes

12 or more carbon atoms

At least 10 carbon atoms and two functional groups

ACPD
11, 26347–26413, 2011

At least six carbon atoms and two functional groups, one of which is an acid

Trifunctional

From the above criteria, 26 species from the chemical mechanism described above that have the potential to produce SOA were selected (Table S1 in the supplementary information). All the species were oxygenated derivatives from aromatics, isoprene, alpha-pinene, limonene and carbonyls.

The partitioning coefficient K_i for each compound listed in Table S1 in the supplementary information is calculated explicitly according to:

$$K_i = \frac{RT}{10^6 MW \zeta_i P^0_{L,i}} \tag{3}$$

Where R (8.206×10^{-5} atm m^3 mol^{-1} K^{-1}) is the ideal gas constant, T (K) the temperature, MW (g mol^1) the average molecular weight of the absorbing aerosol phase, ζ_i (dimensionless) the activity coefficient of the compound in the organic aerosol phase, $P^0_{L,i}$ (atm) the compound vapor pressure and 10^6 is a unit conversion factor (g g^{-1}).

Since experimentally determined vapor pressures are not available for many species, we used the method of Myrdal and Yalkowsky (1997) to determine $P^0_{L,i}$, with some changes added to include the particular chemical structure of the SOA forming compounds (Camredon and Aumont, 2006). The Myrdal and Yalkowsky method estimates the boiling point of a given organic compound based on the Joback group contribution method (Reid et al., 1987), and then estimates the vapor pressure at a given temperature. Similar methods have been used previously by Griffin et al. (2002), Zhang et al. (2004) and Pun et al. (2006). As noted by Barley and McFiggans (2010), the Joback method for estimating boiling points tends to underestimate the amount of material that should partition to the aerosol phase. Thus, we should keep in mind the uncertainties of the vapor-pressure estimates when drawing the conclusions regarding the ability of this mechanism to reproduce observations.

Several authors (e.g. Pankow, 1994a and Kamens et al., 1999) have assumed that the value of ζ is equal to one for a given oxidation product in an aerosol particle

ACPD
11, 26347–26413, 2011

composed of a mixture of similar species. Although methods have been proposed to estimate the activity coefficient (Bowman and Karamalegos, 2002), we set ζ to one for simplicity.

The effect of temperature was taken into account according to the Clausius-Claperron equation using enthalpies of vaporization. However, the values of the enthalpy for most compounds are highly uncertain (Bilde and Pandis, 2001; Chuang and Seinfeld, 2002; Donahue et al., 2006; Stanier et al., 2007; Saathoff et al., 2009; Epstein et al., 2010). In this paper, following other recent studies, we assume the value of 42 kJ mol^{-1} for all organic species for simplicity (Chuang and Seinfeld, 2002; Liao et al., 2007; Heald et al., 2008). Table S1 shows the compounds that are allowed to partition to the aerosol phase, their parent VOC and the partitioning coefficients at a temperature of 298 K.

The molecular weight (MW) used in our formulation remains constant, equal to the MW of the absorbing compounds or set to 150 g mol^{-1} for primary organics. Nevertheless, many laboratory studies of biogenic and anthropogenic SOA formation detected a high MW especially in the presence of oligomers (200–900 g mol^{-1}) (Gross et al., 2006; Sato et al., 2007; Dommen et al., 2006; Iinuma et al., 2007). To incorporate this oligomer formation and other heterogeneous reactions into our model, we treat them in a highly simplified manner by assuming that non-evaporative compounds form with a time constant of 1 day following the reversible gas-particle partitioning process. This 1-day time scale is somewhat arbitrary, but is consistent with the Paulsen et al. (2006) finding. In addition, Vaden et al. (2011) studied the evaporation kinetics of laboratory and ambient SOA, and found that SOA evaporation is very slow, lasting more than a day. More generally, Cappa and Jimenez (2010) analyzed a thermodenuder dataset based on a field study and concluded that a significant fraction of the atmospheric OA consisted of non-evaporative components. Thus, our non-evaporative assumption also agrees well with this conclusion.

The formation of oligomers in heterogeneous reactions within or on aerosols may be reversible or irreversible. Kroll et al. (2005) examined the possible heterogeneous up-

ACPD
11, 26347–26413, 2011

take and irreversible transformation of a number of simple carbonyl species (formaldehyde, octanal, trans-2, 4-hexadienal, glyoxal, methylglyoxal, 2,3-butanedione, 2,4-pentanedione, glutaraldehyde, and hydroxyacetone) onto inorganic seed aerosols. Only glyoxal was reported to substantially increase in the particle phase. Moreover, the lack of particle growth while gas phase glyoxal was still present in their system indicated that the uptake was fully reversible. These results are at odds with those of other researchers (Jang and Kamens, 2001a; Jang et al., 2002, 2003a, 2003b, 2005) who observed significant aerosol growth when inorganic seed was exposed to a wide variety of organic species; compounds studied include simple C4–C10 aldehydes, unsaturated carbonyl compounds, and dicarbonyl compounds.

The time rate of formation of oligomers used in our simple treatment is uncertain, and may vary with different compounds. While some laboratory studies showed that at least some of the oligomers are formed quite rapidly on a time scale of one minute (e.g. Heaton et al., 2007), several chamber studies of the chemical composition, volatility and hygroscopicity of SOA indicated that accretion reactions also take place on longer time scales (Gross et al., 2006; Paulsen et al., 2006; Dommen et al., 2006, Kalberer, et al., 2006). Gross et al., (2006) demonstrated that high MW oligomeric species can be detected within 1 to 2 h (after turning the lights on) due to oligomerization reactions within the aerosol phase. Formation of these low volatility compounds continued for up to 20 h , with about 50–60 % of the SOA particle volume non-volatile at 100 °C for 1,3,5-trimethylbenzene after 5–6 h and 80 to 90 % of the SOA particle volume non-volatile for α-pinene generated SOA after 25 h (Paulsen et al., 2006). The rates of formation of oligomers in the Paulsen et al. study were of order 1 day for 1,3,5-trimethylbenzene and 3 days for a-pinene generated SOA, but might be slower in ambient aerosols, since the oligomer-forming compounds might be more dilute within ambient aerosol mixtures. The rate of formation of oligomers follows a chain growth polymerization model, wherein most of the molecular size develops rapidly followed by a continuous growth in the fraction of SOA that consists of oligomers (Kalberer, et al., 2006). For isoprene in a low NO_x environment, the time constant for formation of low volatility

ACPD
11, 26347–26413, 2011

products within the aerosol phase is about 2.3 days (Chan et al., 2007). In contrast to the Chan et al. study, Domen et al. (2006) observed that particles grew steadily within 8 h mainly due to oligomers formed in the aerosol phase from isoprene photo-oxidation at high NO_x.

Smog chamber experiments have also shown that polymerization within the aerosol phase can be catalyzed by semi-volatile acidic reaction products (Kalberer et al., 2004). The smog-chamber study by Iinuma et al. (2005) examined the effect of acidic seed particles on α-pinene ozonolysis and suggested that acidity promotes SOA formation and increases aerosol yields by up to 40 %. Surratt et al. (2007) examined SOA formation from isoprene and demonstrated that for low relative humidities (30 %), the range of acidities observed in atmospheric aerosols could increase SOA concentrations by a factor of two.

The above discussion demonstrates that oligomer formation seems ubiquitous, but the rate of formation may vary with compound. In addition, the possibility of reversible oligomerization should be considered as well as the dependence of condensed phase reactions on the acidy of the existing aerosols. Nevertheless, our simple 1-day formation rate together with the assumption of irreversibility seems justified at this point in time.

2.2.2 Uptake of glyoxal, methylglyoxal and epoxide

In addition to examining the formation of SOA from the basic Ito et al. (2007) mechanism, we added the formation of SOA from glyoxal, methylglyoxal from the oxidation of several VOC, as well as from epoxide formed in the oxidation of isoprene. Hereafter, we refer to these SOAs as ne_GLYX, ne_MGLY and ne_IEPOX, respectively (see Table 1). Over the past few years, glyoxal and methylglyoxal have gained great attention because of their potential importance to form SOA through aqueous phase reactions due to their high water solubility, their ability to form oligomers via acid catalysis, and their reactivity with OH radicals (Blando and Turpin, 2000; Volkamer et al., 2007; Carlton et al., 2007). Generally, these aqueous-phase reactions can be categorized as radical

ACPD
11, 26347–26413, 2011

or non-radical reactions (Lim et al., 2010). Radical reactions can involve a variety of atmospheric oxidants, including OH radicals, NO_3 radicals, O_3, and can be initiated by photolysis. The chamber study of Volkamer et al. (2009) demonstrated that SOA formation through aqueous photooxidation of glyoxal was dramatic during daytime when the gas-phase OH radicals concentration is about 10^7 molecules cm^{-3}. Non-radical reactions include hemiacetal formation (Liggio et al., 2005a; Loeffler et al., 2006), aldol condensation (Jang et al., 2002), imine formation (Galloway et al., 2009), anhydride formation (Gao et al., 2004), esterification via condensation reactions (Gao et al., 2004), and organosulfate formation (Liggio et al., 2005b; Surratt et al., 2007).

In this paper, we treat the SOA formation from glyoxal, methylglyoxal and epoxide following the basic methods described by Fu et al. (2008, 2009) for glyoxal and methylglyoxal. Based on early laboratory evidence for irreversible surface-controlled uptake of glyoxal to aerosols (Liggio et al., 2005a, b), Fu et al. (2008, 2009) parameterized the loss of gas phase glyoxal and methylglyoxal on aqueous droplets using the following equation:

Where A = total aerosol surface area of aqueous droplets, which we take as the surface area of pure sulfate [cm^2], and C_g is the concentration of gas phase glyoxal or methylglyoxal. The production of aqueous phase products can be directly equated to the loss of gas phase species. The parameter γ is the reactive uptake coefficient, representing the probability that a collision between a gas molecule and the aqueous particle surface will result in irreversible uptake considering processes such as diffusion, mass accommodation, dissolution and chemical reaction. The value of γ was assumed to be the same for glyoxal and methylglyoxal, 2.9×10^{-3}, and we use the same value for epoxide here. In addition to treating uptake on aqueous particles, Fu et al. (2008, 2009) also included uptake by cloud droplets in a similar fashion, but accounting for diffusion limitation. Here, we also account for the uptake by cloud droplets in the same way as that of Fu et al. (2008, 2009).

It should be noted, however, that this simple treatment of irreversible surface-controlled uptake might be misleading if there is competition between reversible vs.

ACPD
11, 26347–26413, 2011

irreversible uptake and bulk reactions vs. surface processes (Ervens and Volkamer, 2010). While the aqueous photooxidation (e.g., aqueous-phase reactions of glyoxal with OH radical) of glyoxal can lead to products that are clearly formed through irreversible processes, Kroll et al. (2005a) and Galloway et al. (2009) report that glyoxal oligomers formed through acid catalyzed pathways are reversible. Furthermore, Ervens and Volkamer (2010) fitted the observed glyoxal loss rates or observed SOA mass formation rates obtained in the literature (i.e. Hastings et al., 2005; Liggio et al., 2005a; Volkamer et al., 2009) to the bulk-limitation equation expressing the SOA formation rate, and showed that the surface area of the aerosol population did not control the uptake of glyoxal and its conversion into SOA mass. In spite of the high uncertainty associated with the processes leading to the SOA formation from glyoxal and methylglyoxal, we use this compact and simplified representation adopted by Fu et al. (2008) to obtain a first order estimate of the significance of glyoxal and methylglyoxal uptake for the total organic aerosols formation rate.

Paulot et al. (2009) demonstrated that isoprene photooxidation under low-NO_x conditions can generate high concentrations of gas-phase epoxydiols , which are then detected in laboratory chamber studies as a key gas-phase intermediate in the formation of SOA from isoprene at low-NOx conditions (Surratt et al., 2010). The reaction kinetics for the formation of epoxydiols have recently been reported (Minerath et al., 2009a, b; Eddingsaas et al., 2010). These studies showed that the acid-catalyzed ring-opening reactions of epoxides in the particle phase were kinetically favorable under typical tropospheric conditions, leading to the formation of known isoprene SOA tracers (e.g., 2-methyltetrols and their corresponding organosulfates) (Surratt et al., 2010). In fact, these isoprene-derived epoxydiols and organosulfates were identified in ambient aerosols during several aircraft measurement campaigns (Froyd et al., 2010; Chan et al., 2010). Therefore, we added the uptake of epoxydiols by sulfate aerosols in the same way as that for glyoxal and methylglyoxal.

ACPD
11, 26347–26413, 2011

2.3 Emissions

Table 2 summarizes the global emissions of gas, aerosols and aerosol precursors used in our model. The emissions of gas-phase species are based on the paper by Ito et al. (2007, 2009) and the POA emissions on the paper by Wang et al. (2009) with some modifications. We include both terrestrial and marine isoprene sources. Terrestrial isoprene emissions are based on a modified version of the inventory of Guenther et al. (1995) by Wang et al. (1998) and Bey et al. (2001), with a global biogenic isoprene source of 470.8 Tg C yr^{-1}. The global marine isoprene emission, with a value of 0.92 Tg C yr^{-1}, is from the estimate by Gantt et al. (2009) based on satellite observations. This total global isoprene flux is then further scaled by monthly mean MODIS chlorophyll concentrations and surface wind speeds to determine the spatial and time variation of the flux (Palmer and Shaw, 2005). The biogenic terpene source is 117.6 Tg C yr^{-1}. The other temperature-dependent BVOC emissions for ethane, propene, acetone, and methanol are distributed according to emissions of isoprene following Ito et al. (2007).

Sources of primary organic emissions in the model include organics from sea spray (35 Tg yr^{-1}), fossil fuel and biofuel emissions (16 Tg yr^{-1}), open biomass burning (47 Tg yr^{-1}). The primary sea spray organic source was estimated using the correlation between chlorophyll-a and the fractional water insoluble organic mass of sea salt following O'Dowd et al. (2008) where the chlorophyll concentrations were those measured by MODIS Aqua averaged for 5 years from 2004 to 2008. The total marine organic aerosol was 35 Tg yr^{-1}, which is very close to the value given by Gantt et al. (2009) based on remote sensing (i.e. 22.3 Tg C yr^{-1} or 35.6 Tg yr^{-1} if the ratio of OM to OC is 1.6). Water soluble organic carbon (WSOC) is also present in marine aerosols and makes up 20–25 % of the total submicron mass (Yoon et al., 2007). It is likely produced through photochemical aging of volatile organic compounds, but has not been included in our analysis because of the large difference in the source strength estimated from "bottom-up" and "top-down" methods (Gantt et al., 2009; Luo and Yu,

ACPD
11, 26347–26413, 2011

2010).

The concentration of the organic portion of the sea salt source was lumped together with the concentration of MSA produced from the oxidation of DMS. For this source, we assumed a pathway based on the reaction of DMS with OH that produced only SO_2 (with a rate coefficient $9.6 \times 10{-}12\exp(-\frac{234}{T})$; and a pathway that forms 0.75 moles of SO_2 and 0.25 moles MSA, with a rate coefficient $k_1 M/(1+2k_2 M)$ where $k_1 = 1.7 \times 10^4 2 \exp\left(\frac{7810}{T}\right)$, and $M = O_2$ (molecules cm^{-3}) following Gondwe et al. (2003) and references therein. The total annual average source of MSA is 8.23 Tg yr^{-1}.

Fossil fuel and biofuel emissions total 16 Tg yr^{-1}. These emissions were estimated by Ito and Penner (2005) for the year 2000, but Wang et al. (2009) adjusted the fossil fuel emissions to fit observed surface BC concentration and we use these emissions here. Open biomass burning emissions total 47.4 Tg yr^{-1} and were developed based on using the Ito and Penner emissions for BC as the an priori estimate together with the inverse model approach of Zhang et al. (2000). The POM associated with open burning was then similarly scaled.

2.4 Dry and wet deposition

As described in Rotman et al. (2004), dry deposition loss rates of gas phase species use the dry deposition algorithm of Wang et al. (1998), which follows the methodology of Wesely et al. (1985). Gravitational settling is taken into account for aerosol species. The settling velocity and the slip correction factor for Stokes law are calculated from Seinfeld and Pandis (1998) using the mass-weighted average radius in each bin for each aerosol component based on the assumed size distribution in each bin. Wet deposition is calculated using the scavenging module developed by Mari et al. (2000) and Liu et al. (2001) which includes scavenging in convective updrafts and first-order rainout and washout in precipitating columns. The horizontal fractional area of each grid box experiencing precipitation is based on the work by Giorgi and Chameides (1986) assuming a cloud liquid water content of 1.5 g m^{-3} for stratiform cloud and

ACPD
11, 26347–26413, 2011

$2.0\,g\,m^{-3}$ for convective cloud. Wet removal of gas-phase organic compounds is calculated based on the Henry's law constant. We adopted Henry's law coefficients for gas-phase species from Ito et al. (2007). The scavenging efficiencies of OA as well as other aerosol types are equal to the mass fraction of OA that is activated to cloud droplets in liquid clouds. The calculation of the fraction is based on the cloud droplet activation parameterization of Abdul-Razzak and Ghan (2000, 2002). The detailed description of the cloud activation is described in Wang and Penner (2009).

3 Results

3.1 Budget calculation

The budget of POA from ocean sources and fossil fuel and biomass burning is shown in Table 3. The atmospheric burden of organics from the oceans is 0.25 Tg, with a lifetime of 2.1 days. This lifetime is somewhat shorter than the lifetime for organics in the standard version of the IMPACT model (Liu et al., 2005), which is 3.2 days, and may reflect the fact that most of the current source only injects POA into the lowest model layer. The total atmospheric burden of fossil and biofuel POA is 0.13 Tg, while that for biomass burning is 0.64 Tg. The lifetime for the surface-based fossil and biofuel emissions is 3.0 days, while that for open burning is 4.9 days.

The global budget of SOA is very uncertain. Recent top-down estimates based either on the mass balance of VOCs or on scaling to the sulfate budget suggest a global source of SOA ranging from 140–910 $Tg\,C\,yr^{-1}$ (Goldstein and Galbally, 2007; Hallquist et al., 2009) corresponding to 280–1820 $Tg\,yr^{-1}$ if the ratio of total OA to OC is 2.0 (Tupin and Lim, 2001). A more recent top-down estimate of the total OA budget using satellite observations of aerosol optical depth and a global model (Heald et al., 2010) was consistent with an SOA source of $150 \pm 120\,Tg\,C\,yr^{-1}$ corresponding to $300 \pm 240\,Tg\,yr^{-1}$ assuming a 2.0:1 OA:OC ratio. In addition, Spracklen et al. (2011) estimate a SOA source ranging from 50 to 230 $Tg\,yr^{-1}$, based on fitting the results

ACPD
11, 26347–26413, 2011

of a global chemical transport model to aerosol mass spectrometer (AMS) observations. In contrast to these top-down estimates, traditional bottom-up estimates from global models that use known or inferred biogenic and /or anthropogenic VOC precursor fluxes together with laboratory data from oxidation experiments give much lower SOA production rates of 14-82 Tg yr^{-1} (Hallquist et al., 2009).

Table 4 summarizes the production and the burden for the three simulations performed in this study. The total production rate of SOA in Simulation A is 114 Tg yr^{-1}. A little more than 66 % of the production rate is approximately evenly split between sources associated with methylglyoxal and epoxide while 21 % is associated with ne_oSOA and 11 % with glyoxal. The introduction of the HO_x recycling mechanism of Peeters et al. (2009) has a large impact on the global SOA burden and production rate. Both the total burden and production rate decrease by about 30 % in comparison to that of Simulation A, whereas the burden in Simulation C is only 8 % smaller than that in Simulation A. This reduction is caused by the competition of the 1, 5- and 1, 6-H shift reactions of the isoprene peroxys with their traditional bimolecular reactions (e.g. reactions with NO and HO_2) which reduces the epoxide formation rate more than it is increased due to the increase in OH and HO_2. A detailed analysis of this competition will be described below. The burden and source in Simulation C lie between those in Simulation A and Simulation B. When comparing with some other global chemical transport models bottom-up estimates (Table 5), our SOA production rates are larger in all simulations, but are well within the range deduced by Heald et al. (2010) and Spracklen et al. (2011). This higher source in our SOA formation mainly comes from the irreversible uptake of gas phase glyoxal, methylglyoxal and IEPOX which were not taken into account in traditional two-product models. Actually, our source of ne_oSOA as indicated in Table 5 is comparable to the SOA sources reported for other models. Table 5 also breaks down the sources into those from anthropogenic emissions and those from biogenic emissions. The dominance of biogenic SOA production also agrees well with previous model results. The fraction of biogenic production in our simulations, 85.2 %–89.0 %, is similar to that from previous models, i.e. typically 80–95 %.

ACPD
11, 26347–26413, 2011

The lifetime of total SOA in the model (5–6 days) is somewhat shorter than that from other models, except the results reported by Utembe et al. (2011). This shorter lifetime is mainly due to the larger removal rate coefficients from wet scavenging. One reason for the larger wet removal rate in our model is that most carbonaceous aerosols are internally mixed with sulfate and are generally hygroscopic except very close to source regions (Liu et al., 2005).

The production rates of compounds that partition to the aerosol phase are summarized in Table S1, as well as the relative contribution (annual mean) of various biogenic and anthropogenic species to the total ne_oSOA. Among these precursors, PRN2, or isoprene-hydroxy-nitrate, makes the greatest contribution to total ne_oSOA (54 %, 45 % and 39 % in Simulation A, B, and C, respectively). PRN2 mainly originates from reaction of RO_2 with NO (Reaction R2), although it may originate from a multitude of species, potentially. The reaction of RO_2 with NO also competes with the isomerization trough the 1,5-H shift or 1,6-H shift. This competition reduces the PRN2 formation rate from the reaction of RO_2 with NO. As a result, the PRN2 SOA production rate is decreased to 8.1 Tg yr^{-1} in Simulation B from 13.4 Tg yr^{-1} in Simulation A. Not surprisingly, the PRN2 production rate in Simulation C is higher than that in Simulation B. The total anthropogenic source of ne_oSOA in Simulation A is 3.7 Tg yr^{-1}, while that from biogenics is 20.8 Tg yr^{-1} (Table 4). The lifetime of ne_oSOA is 8.1 days. This lifetime is much longer than that of the other SOA components. One reason for this longer lifetime is the longer lifetime of the precursors, which make them more likely to be transported to higher altitudes prior to the formation of SOA, where dry and wet deposition are less efficient. The lifetime of gas-phase PRN2, which contributes the most to ne_oSOA, is about 9 h , which is longer than that of glyoxal and methylglyoxal (see Table 6). Another reason for the longer lifetime of ne_oSOA can be related to the temperature dependence of the gas-aerosol partition coefficients (Tsigaridis and Kanakidou, 2003; Hoyle et al., 2007). The lower temperature in the upper atmosphere favors the gas to condense on pre-existing aerosols.

ACPD
11, 26347–26413, 2011

Table 6 shows the budget for the SOA precursors. For simulation A, the model predicts a total methylglyoxal formation rate of 156 $Tg\,yr^{-1}$ from biogenic sources, with 26 $Tg\,yr^{-1}$ from anthropogenic sources and 2.2 $Tg\,yr^{-1}$ from acetone (which is a mixture of anthropogenic and biogenic sources). These may be compared to the source strengths reported by Fu et al. (2008) of 116 $Tg\,yr^{-1}$, 16 $Tg\,yr^{-1}$ and 10 $Tg\,yr^{-1}$, respectively. Loss is primarily through photolysis (97 $Tg\,yr^{-1}$) and reaction with OH (43 $Tg\,yr^{-1}$), followed by the uptake by cloud drops (30 $Tg\,yr^{-1}$) and sulfate aerosols (8 $Tg\,yr^{-1}$). Our reaction with OH and on sulfate aerosols and clouds is a somewhat larger proportion of the total loss rate than that in Fu et al. (2008), and photolysis is somewhat less efficient than of Fu et al. (2008). If we add the HO_x recycling mechanism for isoprene oxidation, we produce less methylglyoxal (Simulation B), which is close to that reported by Fu et al. (2008). More methylglyoxal is again predicted in Simulation C when the rates of the 1,5-H and 1,6-H shift in isoprene radicaly are reduced.

The inclusion of the Peeters et al. (2009) HO_x recycling mechanism in Simulation B increases the rate of production of glyoxal by about 34 % compared to that in simulation A, while decreasing the rates of 1,5-H and 1, 6-H shift increases the glyoxal production rate by about 6 %. The total source of glyoxal from Simulation A is 49 $Tg\,yr^{-1}$. This is similar to the total source of Fu et al. (2008), but the proportion of our source from biogenics (89 %) is much higher than that of Fu et al. (2008) (i.e. 54 %). This source is significantly smaller, however, than the estimate of Stavrakou et al. (2009), 95 – 105 $Tg\,yr^{-1}$, which was based on inverse modeling to fit satellite observations of glyoxal. Because our lifetime of glyoxal is similar to that of Stavrakou et al. (2009) (i.e. 3.0 h vs. 2.5 h), we conclude that our glyoxal production rate may be too low to reproduce the satellite observations. The production rate of glyoxal is also relative low in the other two simulations. The proportion of our sink from the reaction of glyoxal with OH and from the formation of aerosols is higher than that by Fu et al. (2008) in all three simulations.

The only pathway to produce epoxides is Reaction (R3), i.e. the RO_2+HO_2 reaction. The introduction of the Peeters et al. (2009) HO_x recycling pathway decreases the

ACPD
11, 26347–26413, 2011

production of epoxides in spite of the increase in RO_2 and HO_2 concentrations. Most of the epoxides are lost by reaction with OH, and about 20 % reacts on sulfate aerosol to form organic aerosols.

The above secondary organic source gases result in total secondary organic aerosol burdens of 0.151, 0.34, and 0.56 Tg for ne_GLY, ne_MGLY and ne_IEPOX in Simulation A, respectively. The lifetimes of these components are 4.10, 3.217 and 5.516 days, respectively. The inclusion of the Peeters et al. (2009) HO_x recycling mechanism makes the lifetime of ne_GLYX and ne_MGLY slightly shorter while slightly increasing the lifetime of ne_IEPOX. The reason for the shorter aerosol lifetime is related to the shorter lifetimes of the corresponding gas-phase precursors (Table 6). Higher OH concentrations in Simulation B consume glyoxal and methylglyoxal more efficiently so that they have shorter lifetimes. For ne_IEPOX, although its precursor epoxide also has a shorter lifetime when the HOx recycling mechanism is included, the geographical distribution has changed (Fig. 2), with its peak concentration shifting from tropical regions with frequent precipitation to North America and East Asia with less precipitation. This change causes a smaller wet deposition flux of ne_IEPOX.

3.2 Global and vertical distribution

Figures 1 and 2 show the annual mean simulated concentrations of POA and SOA at the surface, respectively. The surface distribution of POA shows high concentrations in areas where significant biomass burning occurs. This pattern is consistent with the global average source from biomass burning contributing as much as 75.1 % of all primary organic aerosols from combustion sources, although motor vehicles and industrial sources are an important source of POA in urban areas. The geographical distribution of SOA also reflects precursor emissions, with large concentrations of biogenic (isoprene) SOA in the tropics and in the southeastern United States. The SOA from gas to particle partitioning (ne_oSOA) shows a surface peak over Africa, which tracks POA to a certain extent. This correspondence between POA and ne_oSOA is related to ne_oSOA formation depending not only on the supply of SOA precursors and

ACPD
11, 26347–26413, 2011

oxidants, but also being influenced by the presence of POA as a partitioning medium. On the other hand, ne_MGLY, ne_GLYX and ne_IEPOX formation are related to the sulfate concentration to some extent, reflected in the strong peaks in their surface distributions near polluted areas in the Northern Hemisphere.

The change of each SOA component and total SOA between Simulation A and Simulations B and C is also shown in Fig. 2. Generally, the introduction of the Peeters et al. (2009) isoprene mechanism decreases ne_oSOA and ne_IEPOX surface concentrations and increase ne_GLYX surface concentrations, which is consistent with the change in global sources as described above. ne_MGLY surface concentrations change very little between Simulation A and Simulations B and C. Most regions show a decrease of total SOA between Simulation B-A consistent with the decreases in ne_oSOA and ne_IEPOX. Slowing the rates of the 1,5-H and 1,6-H shifts in isoprene radicals in Simulation C causes all the surface SOA component surface concentrations to increase compared to Simulation B.

The vertical distribution of POA and SOA is shown in Figs. 1b and 3. The high concentrations of POA and SOA in the tropics near the surface (below 700 hPa) are consistent with the biomass burning sources and the significant SOA formation from biogenic precursors, respectively, as described above. One obvious feature of the ne_oSOA plot is that there is sustained SOA production in the free troposphere due to the relatively long lifetimes of ne_oSOA precursors and the colder temperatures in the free troposphere compared to those at the surface. In addition, the formation of ne_MGLY, ne_GLYX and ne_IEPOX is associated with sulfate, which therefore causes these SOA components to be removed efficiently in the lower troposphere.

ACPD
11, 26347–26413, 2011

4 Comparison with measurements

4.1 Surface measurements

Figure 4a shows a comparison of annual mean model predicted and measured OA concentrations (from March 1996 to February 1999) in the United States for the 48 sites of the Interagency Monitoring of Protected Visual Environments (IMPROVE) network (Malm et al., 2000). Measurement data are reported as organic carbon (OC) in micrograms of carbon per cubic meter, while the model predicts organic mass (OM) concentrations. To convert OM to OC, we use a factor of 1.4 for POA and 1.8 for ne_oSOA. These factors are based on Tupin and Lim (2001) who suggested an average of 1.6 ± 0.2 for OM:OC ratio for urban OA and 2.1 ± 0.2 for more-oxygenated background aerosol. For other SOA components, we converted OM to OC based on their molecular mass and carbon number (i.e. 2.4 for ne_GLYX, 2.0 for ne_MGLY and 1.9 for ne_IEPOX). As shown in Fig. 4a, the simulated concentrations for most of the IMPROV sites are generally within a factor of 2 of the observed concentrations. The annual mean OA concentrations have a mean bias (MB) of $-0.088\,\mathrm{ug\,C\,m^{-3}}$ and a normalized mean bias (NMB) of −5.38 % for Simulation A, a MB of $-0.250\,\mathrm{ugC\,m^{-3}}$ and NMB of −15.32 % for Simulation B, and a MB of $-0.090\,\mathrm{ugC\,m^{-3}}$ and NMB of −5.51 % for Simulation C (Table 7).

Chung and Seinfeld (2002) compared their results with observations from the IMPROVE network and reported that OM concentrations were consistently under-predicted by a factor of 3 or more. Park et al. (2003) showed a small bias (∼20 %) in predicted OC concentrations when compared to IMPROVE sites for the year 1998. Liao et al. (2007) under-predicted OM relative to measurements over the United States with a NMB of −34.2 %. Farina et al. (2010) found that their model under-predicted OM by ∼26 % when compared to the IMPROVE network. This model included the chemical aging of anthropogenic SOA by gas-phase reaction of the SOA component with the hydroxyl radical.

ACPD
11, 26347–26413, 2011

Figure 4b compares the model results to measurements taken in Europe during a one year campaign, performed in 2002–2003 and focused on elemental and organic carbon, as part of the European Monitoring and Evaluation Program (EMEP) (Yttri et al., 2007). Again, we used a scaling factor of 1.4 for POA and 1.8 for ne_oSOA to covert from units of OM to units of OC. In contrast to the comparison with the IMPROVE stations, the results of the model are significantly lower than all of the corresponding observations. The average concentrations observed at EMEP sites, however, are much higher than in the IMPROVE data set, as PM10 measurements were reported at the EMEP sites vs. $PM_{2.5}$ in the IMPROVE network. These large particles are not captured very well by our model. To gain further insight into the reasons for the difference between the model and observations, we examined the results for the summer and winter, respectively (Fig. 5). While SOA dominates OM in the summer, in the winter POA contributes most to OM since isoprene emissions are low. Gelencsér et al. (2007) analyzed the PM2.5 organic aerosol over Europe from the CARBOSOL project and concluded that biomass burning primary emissions were a significant contributor to OC in winter. Therefore a possible reason for the winter-time discrepancy is that the emissions from domestic wood combustion are not fully represented in our emission database. Actually, Gilardoni et al. (2011b) specifically distinguished primary and secondary biomass burning organic carbon from primary and secondary fossil organic carbon as well as biogenic organic carbon by using a combined ^{14}C – macro tracer analysis in Ispra, a site in northern Italy. Here we compare our model results with their analysis in Table 8. Obviously, the primary biomass burning organic carbon is significantly under-represented in the model, which indicates that the contribution of wood burning for residential heating, the main source of biomass burning carbon observed in Ispra (Gilardoni et al., 2011b), is not included in the model. For SOA, the model generally underestimates the observations. The SOA in other European sites, therefore, is likely still underestimated in the model. The underestimation of SOA in Europe may be caused by the underestimation of biogenic VOC emissions in these regions, by the low value of enthalpy that is used to represent the temperature dependence

ACPD
11, 26347–26413, 2011

of gas-particle partitioning efficiency, by a wet scavenging rate that is too high, or by an underrepresentation of SOA formation from anthropogenic sources. It should nevertheless be emphasized that some of the EMEP stations, notably Ispra, are located in topographically pronounced terrain and represent rather localized conditions, which are difficult to quantitatively capture with a global model.

Zhang et al. (2007) present observational SOA data (measured by aerosol mass spectrometry, AMS) from a series of surface measurements at multiple sites in the Northern Hemisphere. The measurements at the various sites were made in different seasons and different years between 2000 and 2006 and were reported for the average of varying durations spanning from 8 to 36 days. In addition, most of the reported measurements were performed in urban locations. Figure 6 compares these SOA mass concentrations with our simulations (the monthly average model results correspond to the months of the observations). The contribution of primary semi-volatile organic compounds to SOA production (Robinson et al., 2007; Pye and Seinfeld, 2010), is simply represented by assuming that one half of the emitted POA evolves to form SOA, because of the substantial uncertainty in the emissions, reaction rates, volatility distribution, and SOA yields of POA (Pye and Seinfeld, 2010; Spracklen et al., 2011). Similar to the above mentioned discrepancies for EMEP sites, the largest deviations from the observations shown in Fig. 6 are the modeled underestimates for urban locations and locations directly downwind of urban areas. Part of this problem is likely related to the low horizontal resolution of the model, which cannot be expected to capture high local concentrations that might later evaporate, although uncertainties in the SOA formation mechanisms are also important. In general, it appears that the model-predicted SOA concentrations are in reasonable agreement with the AMS observations. The NMB for Simulation A is −0.214, −0.022 and 0.105 for urban, urban downwind and rural sites, respectively (see the Table 7). The introduction of the Peeters et al. (2009) isoprene mechanism improves the agreement between predicted and observed SOA concentrations at rural sites giving a NMB of −0.037.

ACPD
11, 26347–26413, 2011

The Zhang et al. (2007) database is limited to the Northern Hemisphere extra-tropics, which are influenced by both anthropogenic and biogenic sources. Observations from more remote forested regions may provide a more stringent test of the biogenic sources represented in the model. Table 9 shows measurements from three different campaigns in tropical forested areas in comparison with the model simulations corresponding to the location and time of measurements. While the typical measurements in the Northern mid latitudes indicate an average of about 2~3 $\mu g\,m^{-3}$ for remote sites (Zhang et al., 2007), these forested regions show a relatively low loading of OM of only ~1 $\mu g\,m^{-3}$. In contrast, the model predicts OM that is about a factor of 3 too high over both West Africa and the Amazon basin and a factor of 2 too high over Borneo, Malaysia. Chen et al. (2009) indicated that biogenic SOA dominated the submicron organic aerosol during the AMAZE 2008 experiment, consistent with our modeling findings. Therefore it seems likely that either the production rate of SOA in the model is too large or the biogenic sources are too strong, although the prediction of POA at this site explains around 10 % of the overestimate. The introduction of the Peeters et al. (2009) HO_x-recycling mechanism improves the model estimate of isoprene, but actually degrades the comparison of OM by a small amount. It furthermore appears from these comparisons that the SOA formation mechanism (e.g. the uptake of glyoxal, methyglyoxal and epoxide) in tropical forests needs to be improved. Trainic et al. (2011) conducted experiments to study the uptake of glyoxal on ammonium sulfate seed aerosols under hydrated conditions over a wide range of relative humidities, (RH from 35 % to 90 %) and found that the reactive uptake rate decreased with increasing RH. The ratio of the final organic aerosol mass to the seed mass at the 50 % RH condition was similar to that found by Liggio et al. (2005a) (who conducted their studies at 49 % RH), but decreased by 57 % when the RH increased from 50 % to 90 %. This trend was attributed to the slower glyoxal oligomerization rate caused by the dilution of the ammonium sulfate aerosol at the higher RH values (Liggio et al., 2005a; Trainic et al., 2011). Thus, the work of Trainic et al. (2011) implies that the uptake coefficient adopted here (which was based on Liggio et al., 2005a) is too high in much of the

ACPD
11, 26347–26413, 2011

tropics where typical RH values are around 90 %. Very recently, Nozière et al. (2011) found that a substantial fraction of 2-methyltetrols is from primary biological origin at Aspvreten, Sweden. These 2-methyltetrols were thought to be important tracers in the reactive uptake of IEPOX to form isoprene SOA under low-NO_x conditions (Surratt et al., 2010). Therefore the Nozière et al. (2011) finding may suggest that the SOA from IEPOX is over-estimated in our mechanism. Amazon basin OC concentrations were also overestimated in the recent study of Gilardoni et al. (2011a), who investigated the composition of fine and coarse aerosols in a Brazilian forest site from February through September 2008. Gilardoni et al. (2011a) reported average $PM_{2.5}$ OM concentrations during the wet season (February–June) of 1.7 $\mu g\, m^{-3}$, larger than the wet season concentrations measured at the same site by Chen et al. (2009) by about 60-80 %. In comparison with these measurements, our simulated concentrations are high by a factor of 2. The Gilardoni et al. (2011a) simulations were based on the TM5 global chemistry transport model and treat SOA as primary species (i.e., they assumed that 15 % of natural terpene emissions form SOA and are directly emitted in the model atmosphere). Thus, these simulations also cannot capture observed OM in tropical regions.

4.2 Vertical profiles

Figure 7a compares the simulated mean vertical profile of OC concentrations and the observed mean profile measured by aircraft off the Coast of Japan during the ACE-Asia campaign from April to May 2001. The measurements were made by two methods (thermal optical analysis and Fourier Transform infrared transmission spectroscopy) and were in excellent agreement (Maria et al., 2003). Heald et al. (2005) compared these measurements with the simulation from the GEOS-Chem global 3-D chemical transport model, and deduced that a large source of organic aerosol in the free troposphere is missing from current models. Here, we show the results of our model for the same month that the measurements were made, but for a different year and consequently with different meteorology than during the measurements. Figure 7a

ACPD
11, 26347–26413, 2011

shows that there are still large discrepancies between the model and the measurements in the free troposphere between the measurement and that simulated by our model, although the magnitude of this discrepancy here is smaller than that reported by Heald et al. (2005) (10–100 times). Dunlea et al. (2009) examined the evolution of Asian aerosols during transpacific transport in the INTEX-B campaign and found no evidence for significant SOA formation in the free troposphere. The AMS aircraft measurements for Asian pollution layers in the INTEX-B campaign showed about an order of magnitude lower OC concentrations in the free troposphere than those measured during the ACE-Asia campaign, so our results compare favorably with the INTEX-B results. Similarly, the aircraft observations during the ITCT-2K4 aircraft campaign, conducted from 9 July to 15 August 2004 out of Portsmouth, New Hampshire, did not suggest a major SOA source in the free troposphere either (Heald et al., 2006). An illustrative comparison of the vertical profile of values from our model for aerosol OC with the measured water-soluble organic carbon (WSOC) from the Particle-Into-Liquid Sampler (PILS) instrument on board the NOAA WP3 aircraft is shown in Fig. 7b. It shows that the model performs reasonably well in the boundary layer (below 2 km), but it still underestimates OC in the free troposphere (2–6 km). The mean observed concentrations were $0.900 \pm 0.187 \mu g\,C\,m^{-3}$ in the free troposphere (Heald et al., 2006), and the corresponding mean model value in Simulation A is $0.574 \pm 0.172 \mu g\,C\,m^{-3}$.

5 Discussion and conclusions

The IMPACT model was used to simulate global SOA formation using three different mechanisms. We accounted for SOA formation from traditional gas-particle partitioning by using the explicit full chemistry scheme instead of the 2-product model. We also included SOA formation from the uptake of gas-phase glyoxal and methlyglyoxal into clouds and aqueous sulfate aerosol following the work of Fu et al. (2008, 2009), and from the uptake of gas-phase epoxides into aqueous sulfate aerosol following the work of Paulot et al. (2009). In addition, we examined the influence of including the HO_x

ACPD
11, 26347–26413, 2011

recycling mechanism in the oxidation of isoprene proposed by Peeters et al. (2009). Our SOA formation mechanisms were evaluated by comparing our global chemical transport model simulations with surface observations from the IMPROVE network in North America and the EMEP in Europe and from a collection of AMS measurements. We also compared our results with vertical profiles of OC from aircraft measurements off East Asia and North America.

The total SOA source in Simulation A was 115.7 Tg yr^{-1}, much larger than that estimated by previous global chemical transport models (see Table 5), but is within the range of recent top-down estimates by satellite observations and AMS measurements (Heald et al., 2010; Spracklen et al., 2011). The SOA formation from biogenic precursors (e.g., isoprene, monoterpenes and etc.) dominates that from anthropogenic sources by a large margin, i.e., the fraction of biogenic SOA is 88 %. However, the production of "biogenic" SOA is strongly linked with anthropogenic components through a variety of mechanisms. In fact, anthropogenic POA emissions can provide an absorptive medium for the condensation of semivolatile species of biogenic origin, and anthropogenic sulfate aerosols can facilitate the conversion of glyoxal, methlyglyoxal and epoxides of biogenic origin to SOA. The formation of SOA from biogenic VOCs is also influenced by anthropogenic emissions of NO_x, not only because these biogenic VOCs will react with NO_x or NO_3 to form SVOCs (e.g. isoprene-hydroxy-nitrate), but also since NO_x competes with HO_2 for peroxy radicals formed in the initial stages of VOC oxidation (e.g., Reactions R1 and R3), leading to changes in functional groups and affecting subsequent reactions. The feedback between anthropogenic emissions and the formation of SOA from biogenic VOCs could have significant implications for future emissions regulations and for predicting the change of organic aerosol in response to future climate change. In order to control emissions contributing to the organic aerosol burden, it is necessary to separate the anthropogenic contribution to SOA formation from the natural background OA (Hoyle et al., 2011). Tsigaridis and Kanakidou (2007) found that the global SOA burden would more than double in 2100 mainly due to the increase in oxidants (O_3, OH and NO_3), as a result of increased anthropogenic pollution,

ACPD
11, 26347–26413, 2011

converting more biogenic VOCs to condensable SOA.

The introduction of the Peeters et al. (2009) HO_x recycling mechanism into the isoprene oxidation scheme has a strong impact on global SOA formation. It decreases the production rate of ne_oSOA, ne_MGLY and ne_IEPOX by about 28 %, 16 % and 65 %, respectively, as a result of the competition between the unimolecular isomerization pathway and the traditional oxidation pathways, i.e. isoprene RO_2 + NO and isoprene RO_2 + HO_2. On the other hand, it increases the SOA production rates from glyoxal by about 65 %. The combination of these effects causes the total SOA source to only decrease by 25 %. When the reaction rates for the 1,5-H and 1,6-H shifts in isoprene radicals are decreased by a factor of 10, the total SOA production rate increases from 87 Tg yr^{-1} to 113 Tg yr^{-1}, very close to that from the simulation A which does not consider the HO_x recycling mechanism. The large difference between the simulations B and C is indicative for the discrepancy between state-of-the-art density functional theories (Peeters et al., 2009) and laboratory measurements (Crounse et al., 2011). These different SOA production rates imply that further laboratory work, field measurements and theoretical studies are needed to better constrain the budgets of the SOA components.

Comparison with the IMPROVE network and with AMS surface measurements in the Northern Hemisphere shows that the model can predict the surface organic aerosol concentrations reasonably well with low normalized mean biases ranging from −15 % to 15 % in rural regions, although we underestimate the surface OC concentrations in Europe due to the underestimation of POA in the winter and of SOA in the summer. The close agreement with measurements contrasts with the under-predictions of observations from the IMPROVE network and AMS surface measurements by other models (Chung and Seinfeld, 2002; Liao et al., 2007; Farina et al., 2010; Utembe et al., 2011; Yu, 2011). However, in contrast to our agreement with observations in the relatively polluted regions of the Northern Hemisphere, in pristine tropical forest regions, the model significantly over-estimates the OM loading compared to AMS measurements. This overestimate is present with and without the HO_x recycling mechanism in

ACPD
11, 26347–26413, 2011

the isoprene oxidation scheme. The relative humidity dependence of glyoxal uptake on ammonium sulfate seed aerosols reported by Trainic et al. (2011) implies that our irreversible reactive uptake rate for glyoxal, methylglyoxal and epoxides may be too fast in humid tropical forested regions. To represent the effects of different reaction rates for glyoxal under different relative humidity conditions, an explicit aqueous-phase reaction scheme (e.g. Lim et al., 2010) is needed. Our overestimation in the Amazon basin differs significantly from predictions in the GEOS-Chem model which underestimated OM (Chen et al., 2009), but is consistent with the TM5 model over-prediction (Gilardoni et al., 2011a). In the free troposphere, the model reproduces the OC observed during the ITCT-2K4 aircraft campaign over the North America relatively well, but clearly underestimates OC observations during ACE-Asia campaign off the coast of Japan. However, the model accurately simulates Asian pollution layers during the INTEX-B campaign.

Supplementary material related to this article is available online at: http://www.atmos-chem-phys-discuss.net/11/26347/2011/acpd-11-26347-2011-supplement.pdf.

Acknowledgements. This project was supported by the *EPA STAR program* (grant #F017324). Any opinions, findings, and conclusions or recommendations expressed in this material are those of the authors and do not necessarily reflect the views of the EPA. Thanks also to Roy Chen for critical help with computers and graphics.

References

Abdul-Razzak, H. and Ghan, S. J.: A parameterization of aerosol activation 2. Multiple aerosol types, J. Geophys. Res., 105, 6837–6844, 2000.

Abdul-Razzak, H. and Ghan, S. J.: A parameterization of aerosol activation – 3. Sectional representation, J. Geophys. Res., 107, 2002.

Barley, M. H. and McFiggans, G.: The critical assessment of vapour pressure estimation

ACPD

11, 26347–26413, 2011

methods for use in modelling the formation of atmospheric organic aerosol, Atmos. Chem. Phys., 10, 749–767, doi:10.5194/acp-10-749-2010, 2010.
Bilde, M. and Pandis, S. N.: Evaporation rates and vapor pressures of individual aerosol species formed in the atmospheric oxidation of alpha- and beta-pinene, Environ. Sci. Technol., 35, 3344–3349, 2001.
Blando, J. D. and Turpin, B. J.: Secondary organic aerosol formation in cloud and fog droplets: a literature evaluation of plausibility, Atmos. Environ., 34, 1623–1632, 2000.
Bowman, F. M. and Karamalegos, A. M.: Estimated effects of composition on secondary organic aerosol mass concentrations, Environ. Sci. Technol., 36, 2701–2707, 2002.
Butler, T. M., Taraborrelli, D., Brühl, C., Fischer, H., Harder, H., Martinez, M., Williams, J., Lawrence, M. G., and Lelieveld, J.: Improved simulation of isoprene oxidation chemistry with the ECHAM5/MESSy chemistry-climate model: lessons from the GABRIEL airborne field campaign, Atmos. Chem. Phys., 8, 4529–4546, doi:10.5194/acp-8-4529-2008, 2008.
Camredon, M. and Aumont, B.: Assessment of vapor pressure estimation methods for secondary organic aerosol modeling, Atmos. Environ., 40, 2105–2116, 2006.
Camredon, M., Aumont, B., Lee-Taylor, J., and Madronich, S.: The SOA/VOC/NOx system: an explicit model of secondary organic aerosol formation, Atmos. Chem. Phys., 7, 5599–5610, doi:10.5194/acp-7-5599-2007, 2007.
Capes, G., Murphy, J. G., Reeves, C. E., McQuaid, J. B., Hamilton, J. F., Hopkins, J. R., Crosier, J., Williams, P. I., and Coe, H.: Secondary organic aerosol from biogenic VOCs over West Africa during AMMA, Atmos. Chem. Phys., 9, 3841–3850, doi:10.5194/acp-9-3841-2009, 2009.
Cappa, C. D. and Jimenez, J. L.: Quantitative estimates of the volatility of ambient organic aerosol, Atmos. Chem. Phys., 10, 5409–5424, doi:10.5194/acp-10-5409-2010, 2010.
Carlton, A. G., Turpin, B. J., Altieri, K. E., Seitzinger, S., Reff, A., Lim, H. J., and Ervens, B.: Atmospheric oxalic acid and SOA production from glyoxal: Results of aqueous photooxidation experiments, Atmos. Environ., 41, 7588–7602, 2007.
Carlton, A. G., Pinder, R. W., Bhave, P. V., and Pouliot, G. A.: To what extent can biogenic SOA be controlled?, Environ. Sci. Technol., 44, 3376–3380, 2010.
Chan, A. W. H., Kroll, J. H., Ng, N. L., and Seinfeld, J. H.: Kinetic modeling of secondary organic aerosol formation: effects of particle- and gas-phase reactions of semivolatile products, Atmos. Chem. Phys., 7, 4135–4147, doi:10.5194/acp-7-4135-2007, 2007.
Chen, Q., Farmer, D. K., Schneider, J., Zorn, S. R., Heald, C. L., Karl, T. G., Guenther, A.,

ACPD
11, 26347–26413, 2011

Allan, J. D., Robinson, N., Coe, H., Kimmel, J. R., Pauliquevis, T., Borrmann, S., Pöschl, U., Andreae, M. O., Artaxo, P., Jimenez, J. L., and Martin, S. T.: Mass spectral characterization of submicron biogenic organic particles in the Amazon Basin, Geophys. Res. Lett., 36, L20806, doi:10.1029/2009gl039880, 2009.

Chung, S. H. and Seinfeld, J. H.: Global distribution and climate forcing of carbonaceous aerosols, J. Geophys. Res., 107, D19, doi:10.1029/2001jd001397, 2002.

Coy, L. and Swinbank, R.: Characteristics of stratospheric winds and temperatures produced by data assimilation, J. Geophys. Res., 102, 25763–25781, 1997.

Coy, L., Nash, E. R., and Newman, P. A.: Meteorology of the polar vortex: Spring 1997, Geophys. Res. Lett., 24, 2693–2696, 1997.

Crounse, J. D., Paulot, F., Kjaergaard, H. G., and Wennberg, P. O.,: Peroxy radical isomerization in the oxidation of isoprene, Phys. Chem. Chem. Phys., 13, 13607–13613, 2011.

Czoschke, N. M., Jang, M., and Kamens, R. M.: Effect of acidic seed on biogenic secondary organic aerosol growth, Atmos. Environ., 37, 4287–4299, 2003.

de Gouw, J. A., Middlebrook, A. M., Warneke, C., Goldan, P. D., Kuster, W. C., Roberts, J. M., Fehsenfeld, F. C., Worsnop, D. R., Canagaratna, M. R., Pszenny, A. A. P., Keene, W. C., Marchewka, M., Bertman, S. B., and Bates, T. S.: Budget of organic carbon in a polluted atmosphere: Results from the New England Air Quality Study in 2002, J. Geophys. Res., 110, D16, doi:10.1029/2004jd005623, 2005.

Dommen, J., Metzger, A., Duplissy, J., Kalberer, M., Alfarra, M. R., Gascho, A., Weingartner, E., Prevot, A. S. H., Verheggen, B., and Baltensperger, U.: Laboratory observation of oligomers in the aerosol from isoprene/NOx photooxidation, Geophys. Res. Lett., 33, L13805, doi:10.1029/2006GL026523, 2006.

Donahue, N. M., Robinson, A. L., and Pandis, S. N.: Atmospheric organic particulate matter: From smoke to secondary organic aerosol, Atmos. Environ., 43, 94–106, 2009.

Donahue, N. M., Robinson, A. L., Stanier, C. O., and Pandis, S. N.: Coupled partitioning, dilution, and chemical aging of semivolatile organics, Environ. Sci. Technol., 40, 2635–2643, 2006.

Dunlea, E. J., DeCarlo, P. F., Aiken, A. C., Kimmel, J. R., Peltier, R. E., Weber, R. J., Tomlinson, J., Collins, D. R., Shinozuka, Y., McNaughton, C. S., Howell, S. G., Clarke, A. D., Emmons, L. K., Apel, E. C., Pfister, G. G., van Donkelaar, A., Martin, R. V., Millet, D. B., Heald, C. L., and Jimenez, J. L.: Evolution of Asian aerosols during transpacific transport in INTEX-B, Atmos. Chem. Phys., 9, 7257–7287, doi:10.5194/acp-9-7257-2009, 2009.

ACPD
11, 26347–26413, 2011

Dzepina, K., Volkamer, R. M., Madronich, S., Tulet, P., Ulbrich, I. M., Zhang, Q., Cappa, C. D., Ziemann, P. J., and Jimenez, J. L.: Evaluation of recently-proposed secondary organic aerosol models for a case study in Mexico City, Atmos. Chem. Phys., 9, 5681–5709, doi:10.5194/acp-9-5681-2009, 2009.

Eddingsaas, N. C., VanderVelde, D. G., and Wennberg, P. O.: Kinetics and products of the acid-catalyzed ring-opening of atmospherically relevant butyl epoxy alcohols, J. Phys. Chem. A, 114, 8106–8113, 2010.

Ervens, B. and Volkamer, R.: Glyoxal processing by aerosol multiphase chemistry: towards a kinetic modeling framework of secondary organic aerosol formation in aqueous particles, Atmos. Chem. Phys., 10, 8219–8244, doi:10.5194/acp-10-8219-2010, 2010.

Farina, S. C., Adams, P. J., and Pandis, S. N.: Modeling global secondary organic aerosol formation and processing with the volatility basis set: Implications for anthropogenic secondary organic aerosol, J. Geophys. Res., 115, D09202, doi:10.1029/2009JD013046, 2010.

Froyd, K. D., Murphy, S. M., Murphy, D. M., de Gouw, J. A., Eddingsaas, N. C., and Wennberg, P. O.: Contribution of isoprene-derived organosulfates to free tropospheric aerosol mass, Pro. Natl. Acad. Sci. USA., 107, 21360–21365, 2010.

Fu, T. M., Jacob, D. J., Wittrock, F., Burrows, J. P., Vrekoussis, M., and Henze, D. K.: Global budgets of atmospheric glyoxal and methylglyoxal, and implications for formation of secondary organic aerosols, J. Geophys. Res., 113, D15303, doi:10.1029/2007JD009505, 2008.

Fu, T. M., Jacob, D. J., and Heald, C. L.: Aqueous-phase reactive uptake of dicarbonyls as a source of organic aerosol over eastern North America, Atmos. Environ., 43, 1814–1822, 2009.

Galloway, M. M., Chhabra, P. S., Chan, A. W. H., Surratt, J. D., Flagan, R. C., Seinfeld, J. H., and Keutsch, F. N.: Glyoxal uptake on ammonium sulphate seed aerosol: reaction products and reversibility of uptake under dark and irradiated conditions, Atmos. Chem. Phys., 9, 3331–3345, doi:10.5194/acp-9-3331-2009, 2009.

Gantt, B., Meskhidze, N., and Kamykowski, D.: A new physically-based quantification of marine isoprene and primary organic aerosol emissions, Atmos. Chem. Phys., 9, 4915–4927, doi:10.5194/acp-9-4915-2009, 2009.

Gao, S., Keywood, M., Ng, N. L., Surratt, J., Varutbangkul, V., Bahreini, R., Flagan, R. C., and Seinfeld, J. H.: Low-molecular-weight and oligomeric components in secondary organic aerosol from the ozonolysis of cycloalkenes and alpha-pinene, J. Phys. Chem. A, 108, 10147–10164, 2004a.

ACPD
11, 26347–26413, 2011

Gao, S., Ng, N. L., Keywood, M., Varutbangkul, V., Bahreini, R., Nenes, A., He, J. W., Yoo, K. Y., Beauchamp, J. L., Hodyss, R. P., Flagan, R. C., and Seinfeld, J. H.: Particle phase acidity and oligomer formation in secondary organic aerosol, Environ. Sci. Technol., 38, 6582–6589, 2004b.

Gelencsér, A., May, B., Simpson, D., Sa'nchez-Ochoa, A., Kasper-Giebl, A., Puxbaum, H., Caseiro, A., Pio, C., and Legrand., M.: Source apportionment of $PM_{2.5}$ organic aerosol over Europe: Primary/secondary, natural/anthropogenic, and fossil/biogenic origin, J. Geophys. Res., 112, D23S04, doi:10.1029/2006JD008094, 2007.

Gilardoni, S., Vignati, E., Cavalli, F., Putaud, J. P., Larsen, B. R., Karl, M., Stenström, K., Genberg, J., Henne, S., and Dentener, F.: Better constraints on sources of carbonaceous aerosols using a combined ^{14}C - macro tracer analysis in a European rural background site, Atmos. Chem. Phys., 11, 5685-5700, doi:10.5194/acp-11-5685-2011, 2011a.

Gilardoni, S., Vignati, E., Marmer, E., Cavalli, F., Belis, C., Gianelle, V., Loureiro, A., and Artaxo, P.: Sources of carbonaceous aerosol in the Amazon basin, Atmos. Chem. Phys., 11, 2747–2764, doi:10.5194/acp-11-2747-2011, 2011b.

Giorgi, F. and Chameides, W. L.: Rainout lifetimes of highly soluble aerosols and gases as inferred from simulations with a g general-circulation model, J. Geophys. Res., 91, 14367–14376, 1986.

Goldstein, A. H. and Galbally, I. E.: Known and unexplored organic constituents in the earth's atmosphere, Environ. Sci. Technol., 41, 1514–1521, 2007.

Goldstein, A. H., Koven, C. D., Heald, C. L., and Fung, I. Y.: Biogenic carbon and anthropogenic pollutants combine to form a cooling haze over the southeastern United States, Proc. Natl. Acda. Sci. USA., 106, 8835–8840, 2009.

Griffin, R. J., Dabdub, D., and Seinfeld, J. H.: Secondary organic aerosol – 1. Atmospheric chemical mechanism for production of molecular constituents, J. Geophys. Res., 107, D17, doi:10.1029/2001JD000541, 2002.

Gross, D. S., Galli, M. E., Kalberer, M., Prevot, A. S. H., Dommen, J., Alfarra, M. R., Duplissy, J., Gaeggeler, K., Gascho, A., Metzger, A., and Baltensperger, U.: Real-time measurement of oligomeric species in secondary organic aerosol with the aerosol time-of-flight mass spectrometer, Anal. Chem, 78, 2130–2137, 2006.

Guenther, A., Hewitt, C. N., Erickson, D., Fall, R., Geron, C., Graedel, T., Harley, P., Klinger, L., Lerdau, M., McKay, W. A., Pierce, T., Scholes, B., Steinbrecher, R., Tallamraju, R., Taylor, J., and Zimmerman, P.: A global-model of natural volatile organic-compound emissions, J.

ACPD
11, 26347–26413, 2011

Geophys. Res., 100, 8873–8892, 1995.
Guenther, A., Karl, T., Harley, P., Wiedinmyer, C., Palmer, P. I., and Geron, C.: Estimates of global terrestrial isoprene emissions using MEGAN (Model of Emissions of Gases and Aerosols from Nature), Atmos. Chem. Phys., 6, 3181–3210, doi:10.5194/acp-6-3181-2006, 2006.
Hallquist, M., Wenger, J. C., Baltensperger, U., Rudich, Y., Simpson, D., Claeys, M., Dommen, J., Donahue, N. M., George, C., Goldstein, A. H., Hamilton, J. F., Herrmann, H., Hoffmann, T., Iinuma, Y., Jang, M., Jenkin, M. E., Jimenez, J. L., Kiendler-Scharr, A., Maenhaut, W., McFiggans, G., Mentel, Th. F., Monod, A., Prvt, A. S. H., Seinfeld, J. H., Surratt, J. D., Szmigielski, R., and Wildt, J.: The formation, properties and impact of secondary organic aerosol: current and emerging issues, Atmos. Chem. Phys., 9, 5155–5236, doi:10.5194/acp-9-5155-2009, 2009.
Hastings, W. P., Koehler, C. A., Bailey, E. L., and De Haan, D. O.: Secondary organic aerosol formation by glyoxal hydration and oligomer formation: Humidity effects and equilibrium shifts during analysis, Environ. Sci. Technol., 39, 8728–8735, 2005.
Heald, C. L., Jacob, D. J., Park, R. J., Russell, L. M., Huebert, B. J., Seinfeld, J. H., Liao, H., and Weber, R. J.: A large organic aerosol source in the free troposphere missing from current models, Geophys. Res. Lett., 32, L18809, doi:10.1029/2005GL023831, 2005.
Heald, C. L., Jacob, D. J., Turquety, S., Hudman, R. C., Weber, R. J., Sullivan, A. P., Peltier, R. E., Atlas, E. L., de Gouw, J. A., Warneke, C., Holloway, J. S., Neuman, J. A., Flocke, F. M., and Seinfeld, J. H.: Concentrations and sources of organic carbon aerosols in the free troposphere over North America, J. Geophys. Res., 111, D23S47, doi:10.1029/2006JD007705, 2006.
Heald, C. L., Henze, D. K., Horowitz, L. W., Feddema, J., Lamarque, J. F., Guenther, A., Hess, P. G., Vitt, F., Seinfeld, J. H., Goldstein, A. H., and Fung, I.: Predicted change in global secondary organic aerosol concentrations in response to future climate, emissions, and land use change, J. Geophys. Res., 113, D05211, doi:10.1029/2007JD009092, 2008.
Heald, C. L., Ridley, D. A., Kreidenweis, S. M., and Drury, E. E.: Satellite observations cap the atmospheric organic aerosol budget, Geophys. Res. Lett., 37, L24808, doi:10.1029/2010GL045095, 2010.
Heaton, K. J., Dreyfus, M. A., Wang, S., and Johnston, M. V.: Oligomers in the early stage of biogenic secondary organic aerosol formation and growth, Environ. Sci. Technol., 41, 6129–6136, 2007.

ACPD
11, 26347–26413, 2011

Henze, D. K. and Seinfeld, J. H.: Global secondary organic aerosol from isoprene oxidation, Geophys. Res. Lett., 33, L09812, doi:10.1029/2006GL025976, 2006.

Henze, D. K., Seinfeld, J. H., Ng, N. L., Kroll, J. H., Fu, T.-M., Jacob, D. J., and Heald, C. L.: Global modeling of secondary organic aerosol formation from aromatic hydrocarbons: high- vs. low-yield pathways, Atmos. Chem. Phys., 8, 2405–2420, doi:10.5194/acp-8-2405-2008, 2008.

Herzog, M., Weisenstein, D. K., and Penner, J. E.: A dynamic aerosol module for global chemical transport models: Model description, J. Geophys. Res., 109, D18202, doi:10.1029/2003JD004405, 2004.

Hodzic, A., Jimenez, J. L., Madronich, S., Canagaratna, M. R., DeCarlo, P. F., Kleinman, L., and Fast, J.: Modeling organic aerosols in a megacity: potential contribution of semi-volatile and intermediate volatility primary organic compounds to secondary organic aerosol formation, Atmos. Chem. Phys., 10, 5491–5514, doi:10.5194/acp-10-5491-2010, 2010.

Hoyle, C. R., Berntsen, T., Myhre, G., and Isaksen, I. S. A.: Secondary organic aerosol in the global aerosol chemical transport model Oslo CTM2, Atmos. Chem. Phys., 7, 5675–5694, doi:10.5194/acp-7-5675-2007, 2007.

Hoyle, C. R., Myhre, G., Berntsen, T. K., and Isaksen, I. S. A.: Anthropogenic influence on SOA and the resulting radiative forcing, Atmos. Chem. Phys., 9, 2715–2728, doi:10.5194/acp-9-2715-2009, 2009.

Hoyle, C. R., Boy, M., Donahue, N. M., Fry, J. L., Glasius, M., Guenther, A., Hallar, A. G., Huff Hartz, K., Petters, M. D., Petj, T., Rosenoern, T., and Sullivan, A. P.: A review of the anthropogenic influence on biogenic secondary organic aerosol, Atmos. Chem. Phys., 11, 321–343, doi:10.5194/acp-11-321-2011, 2011.

Huffman, J. A., Docherty, K. S., Aiken, A. C., Cubison, M. J., Ulbrich, I. M., DeCarlo, P. F., Sueper, D., Jayne, J. T., Worsnop, D. R., Ziemann, P. J., and Jimenez, J. L.: Chemically-resolved aerosol volatility measurements from two megacity field studies, Atmos. Chem. Phys., 9, 7161–7182, doi:10.5194/acp-9-7161-2009, 2009a.

Huffman, J. A., Docherty, K. S., Mohr, C., Cubison, M. J., Ulbrich, I. M., Ziemann, P. J., Onasch, T. B., and Jimenez, J. L.: Chemically-resolved volatility measurements of organic aerosol from different sources, Environ. Sci. Technol., 43, 5351–5357, 2009b.

Iinuma, Y., Boge, O., Gnauk, T., and Herrmann, H.: Aerosol-chamber study of the alpha-pinene/O-3 reaction: influence of particle acidity on aerosol yields and products, Atmos. Environ., 38, 761–773, 2004.

ACPD
11, 26347–26413, 2011

Iinuma, Y., Boge, O., Miao, Y., Sierau, B., Gnauk, T., and Herrmann, H.: Laboratory studies on secondary organic aerosol formation from terpenes, Faraday Discuss., 130, 279–294, 2005.
Iinuma, Y., Muller, C., Boge, O., Gnauk, T., and Herrmann, H.: The formation of organic sulfate esters in the limonene ozonolysis secondary organic aerosol (SOA) under acidic conditions, Atmos. Environ., 41, 5571–5583, 2007.
Ito, A., Sillman, S., and Penner, J. E.: Effects of additional nonmethane volatile organic compounds, organic nitrates, and direct emissions of oxygenated organic species on global tropospheric chemistry, J. Geophys. Res., 112, D06309, doi:10.1029/2005JD006556, 2007.
Ito, A., Sillman, S., and Penner, J. E.: Global chemical transport model study of ozone response to changes in chemical kinetics and biogenic volatile organic compounds emissions due to increasing temperatures: Sensitivities to isoprene nitrate chemistry and grid resolution, J. Geophys. Res., 114, D09301, doi:10.1029/2008JD011254, 2009.
Jang, M. S. and Kamens, R. M.: Characterization of secondary aerosol from the photooxidation of toluene in the presence of NO_x and 1-propene, Environ. Sci. Technol., 35, 3626–3639, 2001.
Jang, M. S., Czoschke, N. M., Lee, S., and Kamens, R. M.: Heterogeneous atmospheric aerosol production by acid-catalyzed particle-phase reactions, Science, 298, 814–817, 2002.
Jang, M., Lee, S., and Kamens, R. M.: Organic aerosol growth by acid-catalyzed heterogeneous reactions of octanal in a flow reactor, Atmos. Environ., 37, 2125–2138, 2003a.
Jang, M. S., Carroll, B., Chandramouli, B., and Kamens, R. M.: Particle growth by acid-catalyzed heterogeneous reactions of organic carbonyls on preexisting aerosols, Environ. Sci. Technol., 37, 3828–3837, 2003b.
Jang, M., Czoschke, N. M., and Northcross, A. L.: Atmospheric organic aerosol production by heterogeneous acid-catalyzed reactions, Chemphyschem, 5, 1647–1661, 2004.
Jang, M. S., Czoschke, N. M., and Northcross, A. L.: Semiempirical model for organic aerosol growth by acid-catalyzed heterogeneous reactions of organic carbonyls, Environ. Sci. Technol., 39, 164–174, 2005.
Jang, M., Czoschke, N. M., Northcross, A. L., Cao, G., and Shaof, D.: SOA formation from partitioning and heterogeneous reactions: Model study in the presence of inorganic species, Environ. Sci. Technol., 40, 3013–3022, 2006.
Jimenez, J. L., Canagaratna, M. R., Donahue, N. M., Prevot, A. S. H., Zhang, Q., Kroll, J. H., DeCarlo, P. F., Allan, J. D., Coe, H., Ng, N. L., Aiken, A. C., Docherty, K. S., Ulbrich, I. M.,

ACPD
11, 26347–26413, 2011

Grieshop, A. P., Robinson, A. L., Duplissy, J., Smith, J. D., Wilson, K. R., Lanz, V. A., Hueglin, C., Sun, Y. L., Tian, J., Laaksonen, A., Raatikainen, T., Rautiainen, J., Vaattovaara, P., Ehn, M., Kulmala, M., Tomlinson, J. M., Collins, D. R., Cubison, M. J., Dunlea, E. J., Huffman, J. A., Onasch, T. B., Alfarra, M. R., Williams, P. I., Bower, K., Kondo, Y., Schneider, J., Drewnick, F., Borrmann, S., Weimer, S., Demerjian, K., Salcedo, D., Cottrell, L., Griffin, R., Takami, A., Miyoshi, T., Hatakeyama, S., Shimono, A., Sun, J. Y., Zhang, Y. M., Dzepina, K., Kimmel, J. R., Sueper, D., Jayne, J. T., Herndon, S. C., Trimborn, A. M., Williams, L. R., Wood, E. C., Middlebrook, A. M., Kolb, C. E., Baltensperger, U., and Worsnop, D. R.: Evolution of Organic Aerosols in the Atmosphere, Science, 326, 1525–1529, 2009.

Johnson, D., Utembe, S. R., and Jenkin, M. E.: Simulating the detailed chemical composition of secondary organic aerosol formed on a regional scale during the TORCH 2003 campaign in the southern UK, Atmos. Chem. Phys., 6, 419–431, doi:10.5194/acp-6-419-2006, 2006.

Kalberer, M., Paulsen, D., Sax, M., Steinbacher, M., Dommen, J., Prevot, A. S. H., Fisseha, R., Weingartner, E., Frankevich, V., Zenobi, R., and Baltensperger, U.: Identification of polymers as major components of atmospheric organic aerosols, Science, 303, 1659–1662, 2004.

Kalberer, M., Sax, M., and Samburova, V.: Molecular size evolution of oligomers in organic aerosols collected in urban atmospheres and generated in a smog chamber, Environ. Sci. Technol., 40, 5917–5922, 2006.

Kamens, R., Jang, M., Chien, C. J., and Leach, K.: Aerosol formation from the reaction of alpha-pinene and ozone using a gas-phase kinetics aerosol partitioning model, Environ. Sci. Technol., 33, 1430–1438, 1999.

Kanakidou, M., Seinfeld, J. H., Pandis, S. N., Barnes, I., Dentener, F. J., Facchini, M. C., Van Dingenen, R., Ervens, B., Nenes, A., Nielsen, C. J., Swietlicki, E., Putaud, J. P., Balkanski, Y., Fuzzi, S., Horth, J., Moortgat, G. K., Winterhalter, R., Myhre, C. E. L., Tsigaridis, K., Vignati, E., Stephanou, E. G., and Wilson, J.: Organic aerosol and global climate modelling: a review, Atmos. Chem. Phys., 5, 1053–1123, doi:10.5194/acp-5-1053-2005, 2005.

Karl, T., Guenther, A., Turnipseed, A., Tyndall, G., Artaxo, P., and Martin, S.: Rapid formation of isoprene photo-oxidation products observed in Amazonia, Atmos. Chem. Phys., 9, 7753–7767, doi:10.5194/acp-9-7753-2009, 2009.

Kleindienst, T. E., Jaoui, M., Lewandowski, M., Offenberg, J. H., Lewis, C. W., Bhave, P. V., and Edney, E. O.: Estimates of the contributions of biogenic and anthropogenic hydrocarbons to secondary organic aerosol at a southeastern US location, Atmos. Environ., 41, 8288–8300, 2007.

ACPD
11, 26347–26413, 2011

Kleinman, L. I., Springston, S. R., Daum, P. H., Lee, Y.-N., Nunnermacker, L. J., Senum, G. I., Wang, J., Weinstein-Lloyd, J., Alexander, M. L., Hubbe, J., Ortega, J., Canagaratna, M. R., and Jayne, J.: The time evolution of aerosol composition over the Mexico City plateau, Atmos. Chem. Phys., 8, 1559–1575, doi:10.5194/acp-8-1559-2008, 2008.

Kroll, J. H., and Seinfeld, J. H.: Chemistry of secondary organic aerosol: Formation and evolution of low-volatility organics in the atmosphere, Atmos. Environ., 42, 3593–3624, 2008.

Kroll, J. H., Ng, N. L., Murphy, S. M., Varutbangkul, V., Flagan, R. C., and Seinfeld, J. H.: Chamber studies of secondary organic aerosol growth by reactive uptake of simple carbonyl compounds, J. Geophys. Res., 110, D23207, doi:10.1029/2005JD006004, 2005.

Kubistin, D., Harder, H., Martinez, M., Rudolf, M., Sander, R., Bozem, H., Eerdekens, G., Fischer, H., Gurk, C., Klpfel, T., Knigstedt, R., Parchatka, U., Schiller, C. L., Stickler, A., Taraborrelli, D., Williams, J., and Lelieveld, J.: Hydroxyl radicals in the tropical troposphere over the Suriname rainforest: comparison of measurements with the box model MECCA, Atmos. Chem. Phys., 10, 9705–9728, doi:10.5194/acp-10-9705-2010, 2010.

Lee-Taylor, J., Madronich, S., Aumont, B., Camredon, M., Hodzic, A., Tyndall, G. S., Apel, E., and Zaveri, R. A.: Explicit modeling of organic chemistry and secondary organic aerosol partitioning for Mexico City and its outflow plume, Atmos. Chem. Phys. Discuss., 11, 17013–17070, doi:10.5194/acpd-11-17013-2011, 2011.

Lelieveld, J., Butler, T. M., Crowley, J. N., Dillon, T. J., Fischer, H., Ganzeveld, L., Harder, H., Lawrence, M. G., Martinez, M., Taraborrelli, D., and Williams, J.: Atmospheric oxidation capacity sustained by a tropical forest, Nature, 452, 737–740, 2008.

Lewis, C. W., Klouda, G. A., and Ellenson, W. D.: Radiocarbon measurement of the biogenic contribution to summertime PM-2.5 ambient aerosol in Nashville, TN, Atmos. Environ., 38, 6053–6061, 2004.

Liao, H., Henze, D. K., Seinfeld, J. H., Wu, S. L., and Mickley, L. J.: Biogenic secondary organic aerosol over the United States: Comparison of climatological simulations with observations, J. Geophys. Res., 112, D06201, doi:10.1029/2006JD007813, 2007.

Liggio, J., Li, S. M., and McLaren, R.: Reactive uptake of glyoxal by particulate matter, J. Geophys. Res., 110, D10304, doi:10.1029/2004JD005113, 2005a.

Liggio, J., Li, S. M., and McLaren, R.: Heterogeneous reactions of glyoxal on particulate matter: Identification of acetals and sulfate esters, Environ. Sci. Technol., 39, 1532–1541, 2005b.

Liu, H. Y., Jacob, D. J., Bey, I., and Yantosca, R. M.: Constraints from Pb-210 and Be-7 on wet deposition and transport in a global three-dimensional chemical tracer model driven by

ACPD
11, 26347–26413, 2011

assimilated meteorological fields, J. Geophys. Res., 106, 12109–12128, 2001.
Liu, X. H. and Penner, J. E.: Effect of Mount Pinatubo H2SO4/H2O aerosol on ice nucleation in the upper troposphere using a global chemistry and transport model, J. Geophys. Res., 107, D12, doi:10.1029/2001JD000455, 2002.
Liu, X. H., Penner, J. E., and Herzog, M.: Global modeling of aerosol dynamics: Model description, evaluation, and interactions between sulfate and nonsulfate aerosols, J. Geophys. Res., 110, D18206, doi:10.1029/2004JD005674, 2005.
Luo, G. and Yu, F.: A numerical evaluation of global oceanic emissions of a-pinene and isoprene, Atmos. Chem. Phys., 10, 2007–2015, doi:10.5194/acp-10-2007-2010, 2010.
Mari, C., Jacob, D. J., and Bechtold, P.: Transport and scavenging of soluble gases in a deep convective cloud, J. Geophys. Res., 105, 22255–22267, 2000.
Maria, S. F., Russell, L. M., Turpin, B. J., Porcja, R. J., Campos, T. L., Weber, R. J., and Huebert, B. J.: Source signatures of carbon monoxide and organic functional groups in Asian Pacific Regional Aerosol Characterization Experiment (ACE-Asia) submicron aerosol types, J. Geophys. Res., 108, D23, doi:10.1029/2003JD003703, 2003.
Martinez, M., Harder, H., Kubistin, D., Rudolf, M., Bozem, H., Eerdekens, G., Fischer, H., Klüpfel, T., Gurk, C., Königstedt, R., Parchatka, U., Schiller, C. L., Stickler, A., Williams, J., and Lelieveld, J.: Hydroxyl radicals in the tropical troposphere over the Suriname rainforest: airborne measurements, Atmos. Chem. Phys., 10, 3759–3773, doi:10.5194/acp-10-3759-2010, 2010.
Minerath, E. C. and Elrod, M. J.: Assessing the potential for diol and hydroxy sulfate ester formation from the reaction of epoxides in tropospheric aerosols, Environ. Sci. Technol., 43, 1386–1392, 2009.
Minerath, E. C., Schultz, M. P., and Elrod, M. J.: Kinetics of the reactions of isoprene-derived epoxides in model tropospheric aerosol solutions, Environ. Sci. Technol., 43, 8133–8139, 2009.
Myrdal, P. B. and Yalkowsky, S. H.: Estimating pure component vapor pressures of complex organic molecules, Ind. Eng. Chem. Res., 36, 2494–2499, 1997.
Ng, N. L., Kroll, J. H., Keywood, M. D., Bahreini, R., Varutbangkul, V., Flagan, R. C., Seinfeld, J. H., Lee, A., and Goldstein, A. H.: Contribution of first- versus second-generation products to secondary organic aerosols formed in the oxidation of biogenic hydrocarbons, Environ. Sci. Technol., 40, 2283–2297, 2006.
Nozière, B., González, N. J.D., Borg-Karlson, A.-K., Pei, Y., Redeby, J. P., Krejci, R., Dom-

ACPD
11, 26347–26413, 2011

men, J., Prevot, A. S. H., and Anthonsen, T.,:, Atmospheric chemistry in stereo: A new look at secondary organic aerosols from isoprene, Geophys. Res. Lett., 38, L11807, doi:10.1029/2011GL047323, 2011.
Odum, J. R., Hoffmann, T., Bowman, F., Collins, D., Flagan, R. C., and Seinfeld, J. H.: Gas/particle partitioning and secondary organic aerosol yields, Environ. Sci. Technol., 30, 2580–2585, 1996.
O'Donnell, D., Tsigaridis, K., and Feichter, J.: Estimating the influence of the secondary organic aerosols on present climate using ECHAM5-HAM, Atmos. Chem. Phys. Discuss., 11, 2407–2472, doi:10.5194/acpd-11-2407-2011, 2011.
Palmer, P. I., and Shaw, S. L.: Quantifying global marine isoprene fluxes using MODIS chlorophyll observations, Geophys. Res. Lett., 32, L09805, doi:10.1029/2005GL022592, 2005.
Pankow, J. F.: An absorption-model of the gas aerosol partitioning involved in the formation of secondary organic aerosol, Atmos. Environ., 28, 189–193, 1994.
Pankow, J. F., and Barsanti, K. C.: The carbon number-polarity grid: A means to manage the complexity of the mix of organic compounds when modeling atmospheric organic particulate matter, Atmos. Environ., 43, 2829–2835, 2009.
Paulot, F., Crounse, J. D., Kjaergaard, H. G., Kurten, A., St Clair, J. M., Seinfeld, J. H., and Wennberg, P. O.: Unexpected epoxide formation in the gas-phase photooxidation of isoprene, Science, 325, 730–733, 2009.
Paulsen, D., Weingartner, E., Alfarra, M. R., and Baltensperger, U.: Volatility measurements of photochemically and nebulizer-generated organic aerosol particles, J. Aerosol. Sci., 37, 1025–1051, 2006.
Peeters, J., Nguyen, T. L., and Vereecken, L.: HOx radical regeneration in the oxidation of isoprene, Phys. Chem. Chem. Phys., 11, 5935–5939, 2009.
Penner, J. E., Chuang, C. C., and Grant, K.: Climate forcing by carbonaceous and sulfate aerosols, Clim. Dynam., 14, 839–851, 1998.
Pun, B. K., Seigneur, C., and Lohman, K.: Modeling secondary organic aerosol formation via multiphase partitioning with molecular data, Environ. Sci. Technol., 40, 4722–4731, 2006.
Pye, H. O. T. and Seinfeld, J. H.: A global perspective on aerosol from low-volatility organic compounds, Atmos. Chem. Phys., 10, 4377–4401, doi:10.5194/acp-10-4377-2010, 2010.
Reid, R. C., Prausnitz, J. M., and Polling, B. E.: The properties of gases and liquids, Hill, New York, USA, 1987.
Robinson, A. L., Donahue, N. M., Shrivastava, M. K., Weitkamp, E. A., Sage, A. M., Grieshop,

ACPD
11, 26347–26413, 2011

A. P., Lane, T. E., Pierce, J. R., and Pandis, S. N.: Rethinking organic aerosols: Semivolatile emissions and photochemical aging, Science, 315, 1259–1262, 2007.

Robinson, N. H., Hamilton, J. F., Allan, J. D., Langford, B., Oram, D. E., Chen, Q., Docherty, K., Farmer, D. K., Jimenez, J. L., Ward, M. W., Hewitt, C. N., Barley, M. H., Jenkin, M. E., Rickard, A. R., Martin, S. T., McFiggans, G., and Coe, H.: Evidence for a significant proportion of Secondary Organic Aerosol from isoprene above a maritime tropical forest, Atmos. Chem. Phys., 11, 1039–1050, doi:10.5194/acp-11-1039-2011, 2011.

Rotman, D. A., Atherton, C. S., Bergmann, D. J., Cameron-Smith, P. J., Chuang, C. C., Connell, P. S., Dignon, J. E., Franz, A., Grant, K. E., Kinnison, D. E., Molenkamp, C. R., Proctor, D. D., and Tannahill, J. R.: IMPACT, the LLNL 3-D global atmospheric chemical transport model for the combined troposphere and stratosphere: Model description and analysis of ozone and other trace gases, J. Geophys. Res., 109, D04303, doi:10.1029/2002JD003155, 2004.

Saathoff, H., Naumann, K.-H., Mhler, O., Jonsson, Å., Hallquist, M., Kiendler-Scharr, A., Mentel, Th. F., Tillmann, R., and Schurath, U.: Temperature dependence of yields of secondary organic aerosols from the ozonolysis of a-pinene and limonene, Atmos. Chem. Phys., 9, 1551–1577, doi:10.5194/acp-9-1551-2009, 2009.

Sato, K., Hatakeyama, S., and Imamura, T.: Secondary organic aerosol formation during the photooxidation of toluene: NO_x dependence of chemical composition, J. Phys. Chem. A., 111, 9796–9808, 2007.

Seinfeld, J. H. and Pandis, S. N.: Atmospheric chemistry and physics: from air pollution to climate change, John Wiley, Hoboken, N. J., 1998.

Sillman, S.: A numerical-solution for the equations of tropospheric chemistry based on an analysis of sources and sinks of odd hydrogen, J. Geophys. Res., 96, 20735–20744, 1991.

Simpson, D., Yttri, K. E., Klimont, Z., Kupiainen, K., Caseiro, A., Gelencser, A., Pio, C., Puxbaum, H., and Legrand, M.: Modeling carbonaceous aerosol over Europe: Analysis of the CARBOSOL and EMEP EC/OC campaigns, J. Geophys. Res., 112, D23S14, doi:10.1029/2006JD008158, 2007.

Slowik, J. G., Brook, J., Chang, R. Y.-W., Evans, G. J., Hayden, K., Jeong, C.-H., Li, S.-M., Liggio, J., Liu, P. S. K., McGuire, M., Mihele, C., Sjostedt, S., Vlasenko, A., and Abbatt, J. P. D.: Photochemical processing of organic aerosol at nearby continental sites: contrast between urban plumes and regional aerosol, Atmos. Chem. Phys., 11, 2991–3006, doi:10.5194/acp-11-2991-2011, 2011.

Song, C., Zaveri, R. A., Alexander, M. L., Thornton, J. A., Madronich, S., Ortega, J. V., Zelenyuk,

ACPD
11, 26347–26413, 2011

A., Yu, X. Y., Laskin, A., and Maughan, D. A.: Effect of hydrophobic primary organic aerosols on secondary organic aerosol formation from ozonolysis of alpha-pinene, Geophys. Res. Lett., 34, L20803, doi:10.1029/2007GL030720, 2007.

Spracklen, D. V., Jimenez, J. L., Carslaw, K. S., Worsnop, D. R., Evans, M. J., Mann, G. W., Zhang, Q., Canagaratna, M. R., Allan, J., Coe, H., McFiggans, G., Rap, A., and Forster, P.: Aerosol mass spectrometer constraint on the global secondary organic aerosol budget, Atmos. Chem. Phys. Discuss., 11, 5699–5755, doi:10.5194/acpd-11-5699-2011, 2011.

Stanier, C. O., Pathak, R. K., and Pandis, S. N.: Measurements of the volatility of aerosols from alpha-piniene ozonolysis, Environ. Sci. Technol., 41, 2756–2763, 2007.

Stavrakou, T., Müller, J.-F., De Smedt, I., Van Roozendael, M., Kanakidou, M., Vrekoussis, M., Wittrock, F., Richter, A., and Burrows, J. P.: The continental source of glyoxal estimated by the synergistic use of spaceborne measurements and inverse modelling, Atmos. Chem. Phys., 9, 8431–8446, doi:10.5194/acp-9-8431-2009, 2009.

Stavrakou, T., Peeters, J., and Müller, J.-F.: Improved global modelling of HOx recycling in isoprene oxidation: evaluation against the GABRIEL and INTEX-A aircraft campaign measurements, Atmos. Chem. Phys., 10, 9863–9878, doi:10.5194/acp-10-9863-2010, 2010.

Stone, D., Evans, M. J., Commane, R., Ingham, T., Floquet, C. F. A., McQuaid, J. B., Brookes, D. M., Monks, P. S., Purvis, R., Hamilton, J. F., Hopkins, J., Lee, J., Lewis, A. C., Stewart, D., Murphy, J. G., Mills, G., Oram, D., Reeves, C. E., and Heard, D. E.: HOx observations over West Africa during AMMA: impact of isoprene and NOx, Atmos. Chem. Phys., 10, 9415–9429, doi:10.5194/acp-10-9415-2010, 2010.

Surratt, J. D., Lewandowski, M., Offenberg, J. H., Jaoui, M., Kleindienst, T. E., Edney, E. O., and Seinfeld, J. H.: Effect of acidity on secondary organic aerosol formation from isoprene, Environ. Sci. Technol., 41, 5363–5369, 2007.

Surratt, J. D., Chan, A. W. H., Eddingsaas, N. C., Chan, M. N., Loza, C. L., Kwan, A. J., Hersey, S. P., Flagan, R. C., Wennberg, P. O., and Seinfeld, J. H.: Reactive intermediates revealed in secondary organic aerosol formation from isoprene, Proc. Natl. Acad. Sci. USA., 107, 6640–6645, 2010a.

Surratt, J. D., Chan, A. W. H., Eddingsaas, N. C., Chan, M. N., Loza, C. L., Kwan, A. J., Hersey, S. P., Flagan, R. C., Wennberg, P. O., and Seinfeld, J. H.: Reactive intermediates revealed in secondary organic aerosol formation from isoprene, P. Natl. Acad. Sci. USA., 107, 6640–6645, 2010b.

Szidat, S., Ruff, M., Perron, N., Wacker, L., Synal, H.-A., Hallquist, M., Shannigrahi, A. S.,

ACPD
11, 26347–26413, 2011

Yttri, K. E., Dye, C., and Simpson, D.: Fossil and non-fossil sources of organic carbon (OC) and elemental carbon (EC) in Göteborg, Sweden, Atmos. Chem. Phys., 9, 1521–1535, doi:10.5194/acp-9-1521-2009, 2009.

Tsigaridis, K. and Kanakidou, M.: Secondary organic aerosol importance in the future atmosphere, Atmos. Environ., 41, 4682–4692, 2007.

Trainic, M., Riziq, A. A., Lavi, A., Flores, J. M., and Rudich, Y.: The optical, physical and chemical properties of the products of glyoxal uptake on ammonium sulfate seed aerosols, Atmos. Chem. Phys. Discuss., 11, 19223–19252, doi:10.5194/acpd-11-19223-2011, 2011.

Utembe, S. R., Cooke, M. C., Archibald, A. T., Shallcross, D. E., Derwent, R. G., and Jenkin, M. E.: Simulating secondary organic aerosol in a 3-D Lagrangian chemistry transport model using the reduced Common Representative Intermediates mechanism (CRI v2-R5), Atmos. Environ., 45, 1604–1614, 2011.

Vaden, T. D., Imre, D., Beranek, J., Shrivastava, M., and Zelenyuk, A.: Evaporation kinetics and phase of laboratory and ambient secondary organic aerosol, P. Natl. Acad. Sci. USA., 108, 2190–2195, 2011.

Volkamer, R., Jimenez, J. L., San Martini, F., Dzepina, K., Zhang, Q., Salcedo, D., Molina, L. T., Worsnop, D. R., and Molina, M. J.: Secondary organic aerosol formation from anthropogenic air pollution: Rapid and higher than expected, Geophys. Res. Lett., 33, L17811, doi:10.1029/2006GL026899, 2006.

Volkamer, R., Martini, F. S., Molina, L. T., Salcedo, D., Jimenez, J. L., and Molina, M. J.: A missing sink for gas-phase glyoxal in Mexico City: Formation of secondary organic aerosol, Geophys. Res. Lett., 34, L19807, doi:10.1029/2007GL030752, 2007.

Wang, M. and Penner, J. E.: Aerosol indirect forcing in a global model with particle nucleation, Atmos. Chem. Phys., 9, 239–260, doi:10.5194/acp-9-239-2009, 2009.

Wang, M. H., Penner, J. E., and Liu, X. H.: Coupled IMPACT aerosol and NCAR CAM3 model: Evaluation of predicted aerosol number and size distribution, J. Geophys. Res., 114, D06302, doi:10.1029/2008JD010459, 2009.

Wang, Y. H., Jacob, D. J., and Logan, J. A.: Global simulation of tropospheric O-3-NOx-hydrocarbon chemistry 1. Model formulation, J. Geophys. Res., 103, 10713–10725, 1998.

Wesely, M. L., Cook, D. R., Hart, R. L., and Speer, R. E.: Measurements and parameterization of particulate sulfur dry deposition over grass, J. Geophys. Res., 90, 2131–2143, 1985.

Xia, A. G., Michelangeli, D. V., and Makar, P. A.: Box model studies of the secondary organic aerosol formation under different HC/NOx conditions using the subset of the

ACPD
11, 26347–26413, 2011

Master Chemical Mechanism for alpha-pinene oxidation, J. Geophys. Res., 113, D10301, doi:10.1029/2007JD008726, 2008.

Yoon, Y. J., Ceburnis, D., Cavalli, F., Jourdan, O., Putaud, J. P., Facchini, M. C., Decesari, S., Fuzzi, S., Sellegri, K., Jennings, S. G., and O'Dowd, C. D.: Seasonal characteristics of the physicochemical properties of North Atlantic marine atmospheric aerosols, J. Geophys. Res., 112, D04206, doi:10.1029/2005JD007044, 2007.

Yttri, K. E., Aas, W., Bjerke, A., Cape, J. N., Cavalli, F., Ceburnis, D., Dye, C., Emblico, L., Facchini, M. C., Forster, C., Hanssen, J. E., Hansson, H. C., Jennings, S. G., Maenhaut, W., Putaud, J. P., and Trseth, K.: Elemental and organic carbon in PM10: a one year measurement campaign within the European Monitoring and Evaluation Programme EMEP, Atmos. Chem. Phys., 7, 5711–5725, doi:10.5194/acp-7-5711-2007, 2007.

Yu, F.: A secondary organic aerosol formation model considering successive oxidation aging and kinetic condensation of organic compounds: global scale implications, Atmos. Chem. Phys., 11, 1083–1099, doi:10.5194/acp-11-1083-2011, 2011.

Zhang, Y., Pun, B., Vijayaraghavan, K., Wu, S. Y., Seigneur, C., Pandis, S. N., Jacobson, M. Z., Nenes, A., and Seinfeld, J. H.: Development and application of the model of aerosol dynamics, reaction, ionization, and dissolution (MADRID), J. Geophys. Res., 109, D01202, doi:10.1029/2003JD003501, 2004.

Zhang, Q., Jimenez, J. L., Canagaratna, M. R., Allan, J. D., Coe, H., Ulbrich, I., Alfarra, M. R., Takami, A., Middlebrook, A. M., Sun, Y. L., Dzepina, K., Dunlea, E., Docherty, K., DeCarlo, P. F., Salcedo, D., Onasch, T., Jayne, J. T., Miyoshi, T., Shimono, A., Hatakeyama, S., Takegawa, N., Kondo, Y., Schneider, J., Drewnick, F., Borrmann, S., Weimer, S., Demerjian, K., Williams, P., Bower, K., Bahreini, R., Cottrell, L., Griffin, R. J., Rautiainen, J., Sun, J. Y., Zhang, Y. M., and Worsnop, D. R.: Ubiquity and dominance of oxygenated species in organic aerosols in anthropogenically-influenced Northern Hemisphere midlatitudes, Geophys. Res. Lett., 34, L13801, doi:10.1029/2007GL029979, 2007.

ACPD
11, 26347–26413, 2011

Table 1. Description of three runs and four SOA components performed in this paper.

Name of runs or SOA components	Description
Simulation A	Based on Ito et al. (2007) chemistry mechanism and epoxide formation from isoprene from Paulot et al. (2009), without HO_x recycling.
Simulation B	Includes the mechanism in Simulation A with some reactions modified in accord with the recent literature and HO_x regeneration through isoprene oxidation proposed by Peeters et al. (2009).
Simulation C	The same chemistry mechanism as Simulation B, but with a reduced rate for the 1,5-H and 1,6-H shifts in isoprene radicals by a factor of 10.
ne_oSOA	SOA formed from the traditional gas-particle partitioning of SVOCs produced by oxidation of VOCs. It includes 23 species in Simulation A, and 26 species in Simulation B and C (see the Table S1).
ne_GLYX	Glyoxal SOA formed from the irreversible uptake of gas-phase glyoxal into aqueous sulfate and clouds following the methods used in Fu et al. (2008, 2009).
ne_MGLY	Methylglyoxal SOA formed from the irreversible uptake of gas-phase methylglyoxal into aqueous sulfate and clouds following the methods used in Fu et al. (2008, 2009).
ne_IEPOX	Epoxide SOA fromed from the irreversible uptake of gas-phase epoxide into aqueous sulfate with the same uptake coefficient as glyoxal and methylglyoxal.

ACPD
11, 26347–26413, 2011

Table 2. Global emissions of gases, aerosols and aerosol precursors.

Species	Emission Rate
SO_2 or precursor	92.19 Tg S yr^{-1}
Fossil fuel and industry	61.3 Tg S yr^{-1}
Volcanoes	4.79 Tg S yr^{-1}
DMS	26.1 Tg S yr^{-1}
NO	42.08 Tg N yr^{-1}
Fossil Fuel	22.65 Tg N yr^{-1}
Biomass burning	9.32 Tg N yr^{-1}
Soil	5.52 Tg N yr^{-1}
Lighting	3.0 Tg N yr^{-1}
Aircraft	0.85 Tg N yr^{-1}
Ship	0.74 Tg N yr^{-1}
CO	426 Tg C yr^{-1}
MEK(>C3 ketones)	5.76 Tg C yr^{-1}
PRPE(> = C4 alkenes)	11.3 TgC/yr
C_2H_6	9.27 Tg C yr^{-1}
C_3H_8	7.28 Tg C yr^{-1}
ALK4(>=C4 alkanes)	15.3 Tg C yr^{-1}
Acetaldehyde	3.28 Tg C yr^{-1}
CH_2O	2.35Tg C yr^{-1}
ALK7(C6-C8 alkanes)	11.34Tg C yr^{-1}
Benzene	3.19 Tg C yr^{-1}
Toluene	5.84 Tg C yr^{-1}
Xylene	3.86 Tg C yr^{-1}
trans-2-butene	6.58 Tg C yr^{-1}
HCOOH	2.55 Tg C yr^{-1}
acetic acid	12.43 Tg C yr^{-1}

ACPD
11, 26347–26413, 2011

Table 2. Continued.

Phenol	4.30Tg C yr^{-1}
Ocean source of POA	34.48 Tg yr^{-1}
DMS source of MSA	8.23 Tg yr^{-1}
Fossil fuel+biofuel POA	15.67 Tg OM/yr
Fossil fuel BC	5.80 Tg BC yr^{-1}
Biomass burning OC	47.38 Tg OM/yr
Biomass burning BC	4.71 Tg BC yr^{-1}
Isoprene	472 Tg C yr^{-1}
a-pinene	78.8 Tg C yr^{-1}
Limonene	38.8 Tg C yr^{-1}
PRPE(> = C4 alkenes)	24.2 Tg C yr^{-1}
Methanol	42.9 Tg C yr^{-1}
Acetone	44.54 Tg C yr^{-1}
Ethane	28.18 Tg C yr^{-1}

ACPD
11, 26347–26413, 2011

Table 3. Global budgets for organic aerosols from oceans and primary sources (Tg yr^{-1}).

	This Work
POA from oceans	
Formation of MSA from DMS	8.23
Primary organics from sea spray	34.85
Dry deposition	5.11
Wet deposition	37.94
Burden	0.25
Lifetime (days)	2.10
Anthropogenic POA	
Fossil/bio fuel emission	15.67
Dry deposition	1.49
Wet deposition	14.17
Burden	0.13
Lifetime	3.03
Open biomass burning POA	
Open burning emission	47.38
Dry deposition	3.70
Wet deposition	43.66
Burden	0.64
Lifetime	4.93

ACPD
11, 26347–26413, 2011

Table 4. The global burden, production and lifetime for each SOA component.

		ne_oSOA	ne_GLYX	ne_MGLY	ne_IEPOX	Total SOA
Burden (Tg)	Simulation A	0.54	0.15	0.34	0.56	1.59
	Simulation B	0.39	0.19	0.26	0.20	1.04
	Simulation C	0.62	0.20	0.30	0.35	1.47
Total production (Tg yr^{-1})	Simulation A	24.5	13.5	38.3	37.2	113.5
	Simulation B	17.8	22.2	32.1	12.9	85.0
	Simulation C	26.6	22.6	36.9	25.1	111.2
Anthropogenic production (Tg yr^{-1})	Simulation A	3.7	2.5	5.9	0.0	12.1
	Simulation B	3.4	2.7	6.6	0.0	12.7
	Simulation C	3.6	2.6	6.4	0.0	12.6
Biogenic production (Tg yr^{-1})	Simulation A	20.8	11.0	32.4	37.2	101.4
	Simulation B	14.4	19.5	25.6	12.9	72.4
	Simulation C	23.0	20.0	30.5	25.1	98.6
Lifetime (days)	Simulation A	8.1	4.1	3.2	5.5	5.1
	Simulation B	8.0	3.1	3.0	5.7	4.5
	Simulation C	8.5	3.2	3.0	5.1	4.8

ACPD
11, 26347–26413, 2011

Table 5. Global modeling studies of SOA precursor emission, SOA production, burden and lifetime (Eb: emissions of biogenic species (i.e. isoprene and monoterpenes); Ea: emissions of anthropogenic species (i.e. aromatics); Pb: SOA production from biogenic species; Pa: SOA production from anthropogenic species; Pt and Bt: total SOA production and SOA burden).

References	Global Model	SOA model	Eb (Tg yr^{-1})	Ea (Tg yr^{-1})	Pb (Tg yr^{-1})	Pa (Tg yr^{-1})	Pt (Tg yr^{-1})	Bt (Tg)	Lifetime (day)
O'Donnell et al. (2011)	ECHAM5-HAM	2-product	537	17	21.0	5.6	26.6	0.83	11.4
Heald et al. (2008)	CAM3	2-product	539[a]	16[a]	22.9[a]	1.4[a]	24.3[a]	0.59[a]	8.9
Farina et al. (2010)	GISS II	Volatility basis	736	49	27.28	1.62–11.02[b]	28.9–38.3[b]	0.54–0.98[b]	6.8–9.4[b]
Utembe et al. (2011)	STOCHEM	explicit chemistry	628	60	21.1	1.4	22.5	0.23	3.7
Hoyle et al. (2009)	Oslo CTM3	2-product	386[a]	21.6[a]	–	–	53.4–68.8[c]	0.50-0.7[c]	3.4-3.7[c]
Tsigaridis and Kanakidou (2007)	TM3	2-product	747.2	15.8	16.8	1.8	18.6	0.82	16.0
Henze et al. (2008)	GEOS-Chem	2-product	635.2	18.8	26.8	3.5	30.3	0.81	9.8
This work	IMPACT	explicit chemistry	589.6[a]	12.9[a]	72.4–101.4	12.1–12.7	85.0–113.5	1.04–1.59	4.5–5.1

[a] reported in Tg carbon

[b] high estimate assumes chemical aging of anthropogenic SOA

[c] high estimate assumes partitioning with sulfate

ACPD
11, 26347–26413, 2011

Table 6. Budgets for secondary organic aerosol precursors reacting on acidic aerosols and cloud drops ($Tg\,yr^{-1}$).

Glyoxal				
	Simulation A	Simulation B	Simulation C	Other work
Total sources	48.97	65.72	70.12	95–105 Stavrakou et al. (2009)
Biogenic sources	39.95	57.78	62.16	24.28 Fu et al. (2008)
Anthropogenic sources	9.02	7.94	7.96	20.47 Fu et al. (2008)
Sinks				
Reaction with OH	9.97	15.28	14.79	6.5 Fu et al. (2008)
Reaction with NO3	0.02	0.03	0.03	< 0.1 Fu et al. (2008)
photolysis	23.05	22.89	27.57	28 Fu et al. (2008)
Aerosol formation on cloud drops	10.35	16.90	17.84	5.5 Fu et al. (2008)
Aerosol formation on sulfate aerosols	3.19	5.32	4.82	0.94 Fu et al. (2008)
Wet deposition	1.57	3.21	3.14	1.9 Fu et al. (2008)
Dry deposition	0.86	2.11	1.93	2.2 Fu et al. (2008)
Burden	0.0170	0.020	0.022	0.015 Fu et al. (2008)
Lifetime (hour)	3.04	2.66	2.75	2.9 Fu et al. (2008)
Methylglyoxal				
	Simulation A	Simulation B	Simulation C	Fu et al. (2008)
Total sources	184.5	143.2	167.6	131.8
Biogenic sources	156.3	114.3	138.7	115.6
Anthropogenic sources	26.0	25.6	25.9	16.2
Acetone	2.2	3.3	3.0	10
Sinks				
Reaction with OH	43.0	43.6	45.5	15
Reaction with NO3	9.59×10^{-2}	7.04×10^{-2}	8.31×10^{-2}	< 0.1
photolysis	97.2	62.7	80.0	100
Aerosol formation on cloud drops	30.4	24.6	29.1	14
Aerosol formation on sulfate aerosols	7.9	7.5	7.8	1.4
Wet deposition	3.1	2.8	3.2	1.8
Dry deposition	1.8	1.9	2.0	1.7
Burden	0.037	0.027	0.032	0.025
Lifetime (hours)	1.76	1.65	1.67	1.6
Epoxides from isoprene				
	Simulation A	Simulation B	Simulation C	
Formation of IEPOX	195.2	78.5	150.7	
Sinks				
reaction with OH	157.9	65.8	125.5	
Converted to SOA	37.2	12.9	25.1	
Burden	0.259	0.063	0.145	
Lifetime (hour)	11.62	7.03	8.43	

ACPD
11, 26347–26413, 2011

Table 7. Summary normalized mean bias (NMB) for model evaluation.

		AMS measurements Zhang et al. (2007)		
Simulation name	IMPROVE network	Urban sites	Urban downwind sites	Rural sites
Simulation A	−5.4 %	−21.4 %	−2.2 %	10.5 %
Simulation B	−15.3 %	−38.4 %	−25.4 %	−3.7 %
Simulation C	−5.5 %	−30.3 %	−10.5 %	5.3 %

ACPD
11, 26347–26413, 2011

Table 8. Comparison of simulated seasonal average carbon concentrations (in $\mu g\,C\,m^{-3}$) with the observations made in Ispra from Gilardoni et al. (2011b). POC_bb: primary organic carbon from biomass burning; POC_ff: primary organic carbon from fossil fuel; SOC_bio: secondary organic carbon from oxidation of biogenic species; SOC_ff: secondary organic carbon from fossil fuel.

Source	Winter (Jan–Mar Oct–Dec)				Summer (Apr–Sep)			
	Observation	Simulation A	Simulation B	Simulation C	Observation	Simulation A	Simulation B	Simulation C
POC_bb	11.9	0.02	0.02	0.02	0.5	0.04	0.04	0.04
POC_ff	1.2	0.82	0.82	0.82	0.6	0.34	0.34	0.34
SOC_bio	2.0	0.13	0.12	0.13	3.1	1.41	1.19	1.43
SOC_ff	2.3	0.25	0.25	0.25	1.3	0.22	0.18	0.20

ACPD
11, 26347–26413, 2011

Table 9. Comparison of simulated OA with observed OA measured in tropical forested regions.

		Observations	Simulation A	Simulation B	Simulation C
West Africa		1.18			
(below 2 km)	Total OM ($\mu g\,m^{-3}$)	Capes et al. (2009)	4.78	4.12	5.04
	POA ($\mu g\,m^{-3}$)	–	0.57	0.57	0.57
	ne_oSOA ($\mu g\,m^{-3}$)	–	0.70	0.51	0.79
	ne_GLYX ($\mu g\,m^{-3}$)	–	0.49	1.08	1.03
	ne_MGLY ($\mu g\,m^{-3}$)	–	1.59	1.45	1.63
	ne_IEPOX ($\mu g\,m^{-3}$)	–	1.43	0.51	1.02
	Isoprene (ppt)	620	1734	845	1126
		Capes et al. (2009)			
	NO_x (ppb)	0.21	0.34	0.37	0.35
		Capes et al. (2009)			
Amazon basin		0.70			
(surface)		Chen et al. (2009)			
Total OM ($\mu g\,m^{-3}$)		1.70	3.23	3.45	3.99
		Gilardoni et al. (2011a)			
	POA ($\mu g\,m^{-3}$)	–	0.36	0.36	0.36
	ne_oSOA ($\mu g\,m^{-3}$)	–	0.31	0.25	0.37
	ne_GLYX ($\mu g\,m^{-3}$)	–	0.24	0.95	0.87
	ne_MGLY ($\mu g\,m^{-3}$)	–	1.20	1.49	1.57
	ne_IEPOX ($\mu g\,m^{-3}$)	–	1.12	0.40	0.82
	Isoprene (ppb)	2.0	4.44	1.92	2.69
		Chen et al. (2009)			
Malaysian Borneo		0.74			
(surface)	Total OM ($\mu g\,m^{-3}$)	Robinson et al. (2011)	1.46	1.16	1.49
	POA ($\mu g\,m^{-3}$)	–	0.25	0.25	0.25
	ne_oSOA ($\mu g\,m^{-3}$)	–	0.08	0.06	0.09
	ne_GLYX ($\mu g\,m^{-3}$)	–	0.15	0.32	0.34
	ne_MGLY ($\mu g\,m^{-3}$)	–	0.45	0.40	0.47
	ne_IEPOX ($\mu g\,m^{-3}$)	–	0.53	0.13	0.34

ACPD
11, 26347–26413, 2011

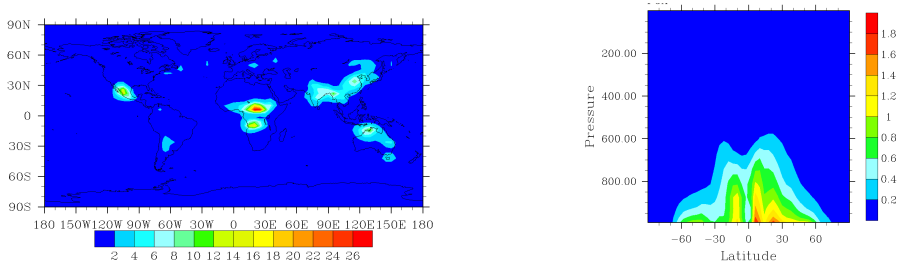

Fig. 1. Annual mean simulated surface POA concentrations (left) and zonal distrutubion of POA concentrations (right). Units: $\mu g\, m^{-3}$.

ACPD
11, 26347–26413, 2011

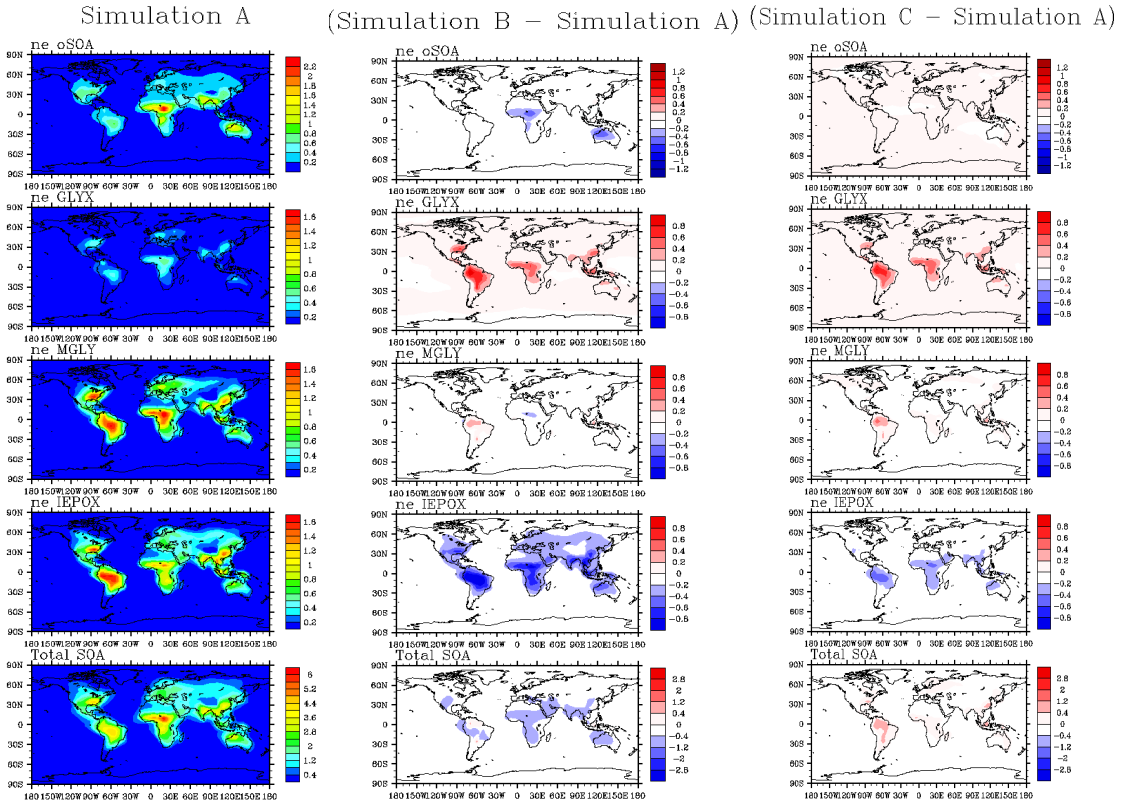

Fig. 2. Annual mean simulated surface SOA concentrations in Simulation A (first column) and the changes in surface SOA concentrations from Simulation A after including the new HO_x recycling mechanism (Simulation B-Simulation A) in the second column, and reducing the reaction rates of 1,5-H and 1,6-H shifts by a factor 10 (Simulation C- Simulation A) in the third column for each SOA component (the first 4 rows) and the total SOA (the fifth row). The maximum and minimum values for color scales in the second and third column are set to half the maximum values of those in the first column (Simulation A). Units: $\mu g\, m^{-3}$.

ACPD
11, 26347–26413, 2011

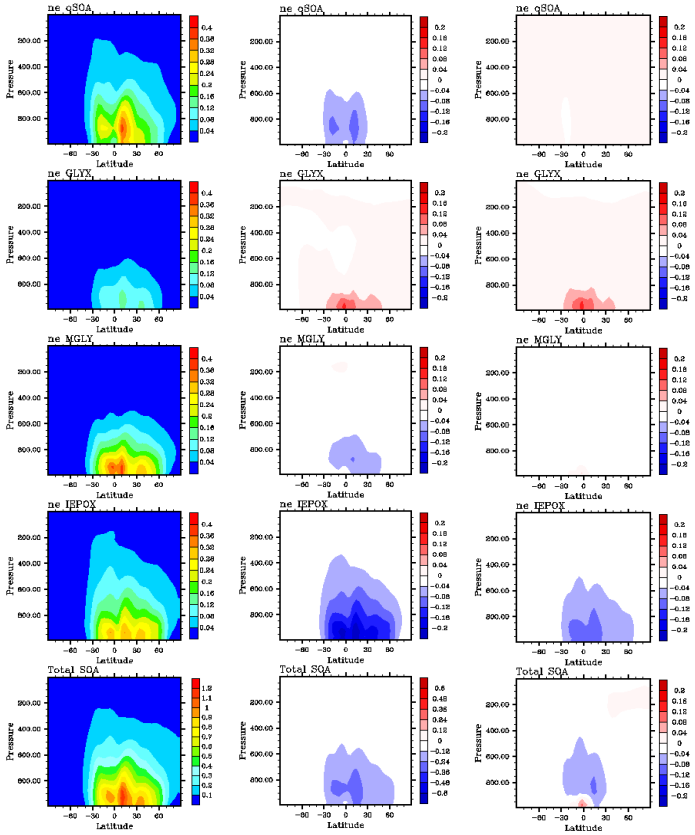

Fig. 3. Annual zonal mean simulated SOA concentrations in Simulation A (first column) and the changes in vertical distributions of SOA concentrations from Simulation A after including the new HO_x recycling mechanism (Simulation B- Simulation A) in the second column, and reducing the reaction rates of 1,5-H and 1,6-H shifts by a factor 10 (Simulation C- Simulation A) in the third column for each SOA component (the first 4 rows) and the total SOA (the fifth row). The maximum and minimum values for color scales in the second and third column are set to half the maximum values of those in the first column (Simulation A). Units: $\mu g\,m^{-3}$.

ACPD
11, 26347–26413, 2011

Global mechanistic model of SOA formation

G. Lin et al.

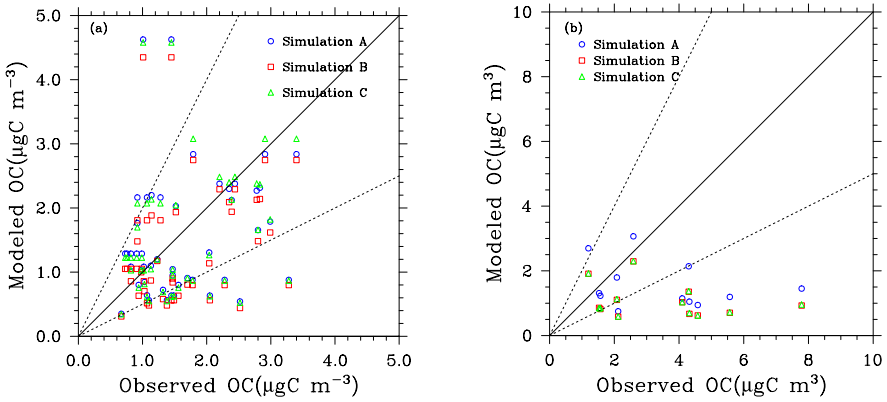

Fig. 4. Total annual averaged organic aerosol model comparison with the IMPROVE **(a)** and EMEP **(b)** observation networks. The solid lines represent ideal agreement (1:1 ratio), and the dashed lines are the 2:1 and 1:2 ratios, i.e. indicating agreement within a factor of 2. The IMPROVE network data are from 1996 to 1999, and the EMEP measurements were made in 2002–2003. The meteorology data used to run the model were for 1997.

ACPD
11, 26347–26413, 2011

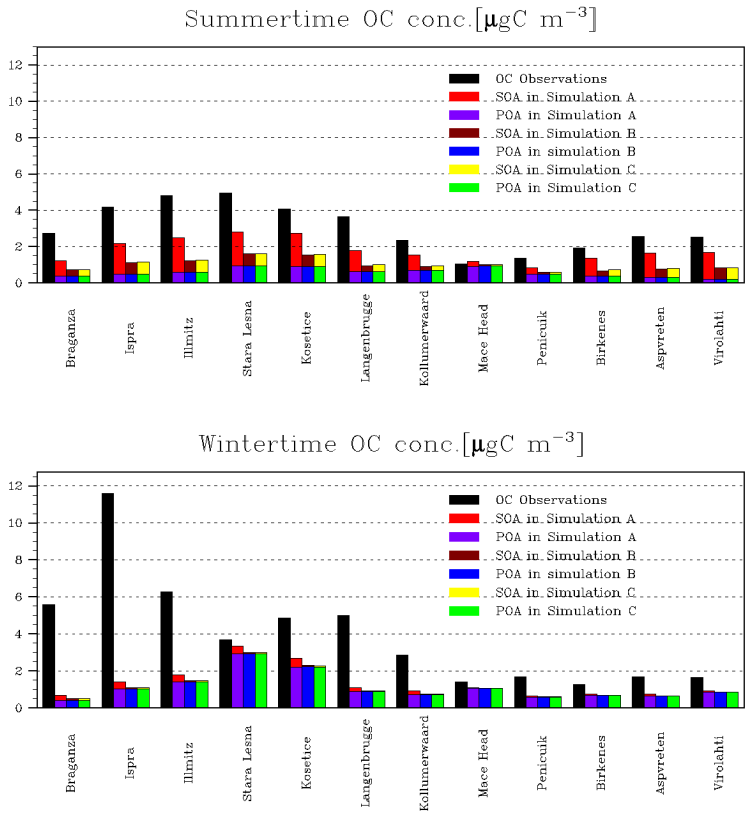

Fig. 5. nOC concentrations in summer (July 2002–October 2002 and April 2003–July 2003) and winter (October 2002-April 2003) for 12 rural sites in the EMEP network. Y axis: OC concentration; X axis: site names (the sites are ordered according to the latitude from the left (the most southern) to the right (the most northern).

ACPD
11, 26347–26413, 2011

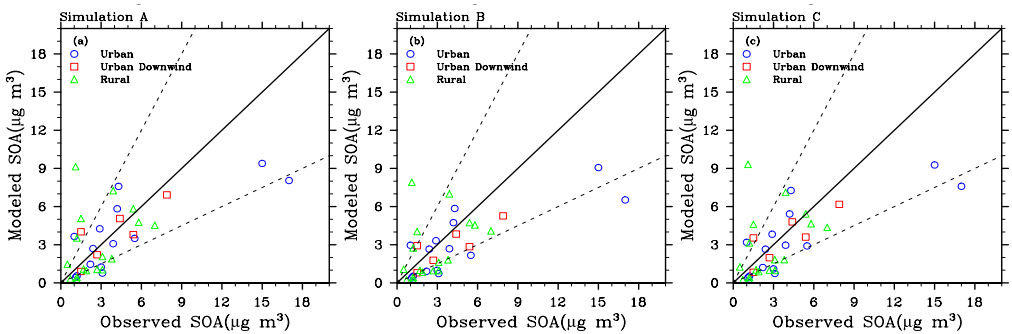

Fig. 6. Comparison of SOA mass concentrations observed at the urban, urban-downwind and rural sites reported in Zhang et al. (2007) with those simulated in Simulation A **(a)**, Simulation B **(b)** and Simulation C **(c)**. Solid lines show the 1:1 ratio, and the dashed lines show the ratios of 1:2 and 2:1. The measurements at the various sites were made in different seasons and different years between 2000 and 2006 and were reported for the average of varying durations spanning from 8 to 36 days. The model results are the average values over the same months as the observations.

ACPD
11, 26347–26413, 2011

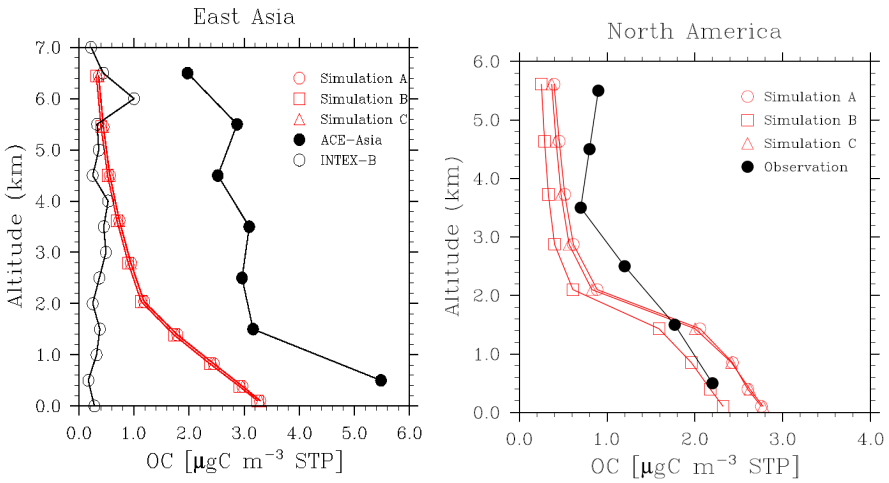

Fig. 7. Mean vertical profiles of total organic carbon at standard conditions of temperature and pressure. Observed mean profiles (black solid circle) were measured during the ACE-Asia campaign at Fukue Island off the coast of Japan in April/MAY 2001 (left plot) and during the ITCT-2K4 aircraft campaign over NE North America which took place in the Summer (July to August) 2004 (right plot). The black empty circles in the left plot represent average vertical profile of aerosol species for Asian pollution layers measured during the INTEX-B campaign made during April to May in 2006. The model results are the average values over the months of the campaigns.

ACPD
11, 26347–26413, 2011